Molecular Plant
Research Article

CellPress
PARTNER JOURNAL

Translational Regulation of Plant Response to High Temperature by a Dual-Function tRNA^{His} Guanylyltransferase in Rice

Ke Chen[1,2,6], Tao Guo[1,6], Xin-Min Li[1,6], Yi-Min Zhang[1,2], Yi-Bing Yang[1,2], Wang-Wei Ye[1], Nai-Qian Dong[1], Chuan-Lin Shi[1,2], Yi Kan[1,2], You-Huang Xiang[1,2], Hai Zhang[1,3], Ya-Chao Li[1,3], Ji-Ping Gao[1], Xuehui Huang[5], Qiang Zhao[4], Bin Han[2,3,4], Jun-Xiang Shan[1,*] and Hong-Xuan Lin[1,2,3,*]

[1]National Key Laboratory of Plant Molecular Genetics, CAS Centre for Excellence in Molecular Plant Sciences and Collaborative Innovation Center of Genetics & Development, Shanghai Institute of Plant Physiology & Ecology, Shanghai Institute for Biological Sciences, Chinese Academic of Sciences, Shanghai 200032, China

[2]University of the Chinese Academy of Sciences, Beijing 100049, China

[3]School of Life Science and Technology, ShanghaiTech University, Shanghai 201210, China

[4]National Center for Gene Research, CAS Center for Excellence in Molecular Plant Sciences, Shanghai Institute of Plant Physiology and Ecology, Shanghai Institutes for Biological Sciences, Chinese Academy of Sciences, Shanghai 200233, China

[5]College of Life and Environmental Sciences, Shanghai Normal University, Shanghai 200234, China

[6]These authors contributed equally to this article.

***Correspondence: Jun-Xiang Shan (jxshan@sibs.ac.cn), Hong-Xuan Lin (hxlin@sibs.ac.cn)**

https://doi.org/10.1016/j.molp.2019.04.012

ABSTRACT

As sessile organisms, plants have evolved numerous strategies to acclimate to changes in environmental temperature. However, the molecular basis of this acclimation remains largely unclear. In this study we identified a tRNA^{His} guanylyltransferase, AET1, which contributes to the modification of pre-tRNA^{His} and is required for normal growth under high-temperature conditions in rice. Interestingly, AET1 possibly interacts with both RACK1A and eIF3h in the endoplasmic reticulum. Notably, AET1 can directly bind to *OsARF* mRNAs including the uORFs of *OsARF19* and *OsARF23*, indicating that AET1 is associated with translation regulation. Furthermore, polysome profiling assays suggest that the translational status remains unaffected in the *aet1* mutant, but that the translational efficiency of *OsARF19* and *OsARF23* is reduced; moreover, OsARF23 protein levels are obviously decreased in the *aet1* mutant under high temperature, implying that AET1 regulates auxin signaling in response to high temperature. Our findings provide new insights into the molecular mechanisms whereby AET1 regulates the environmental temperature response in rice by playing a dual role in tRNA modification and translational control.

Key words: rice, translation regulation, tRNA modification, auxin signaling, environmental temperature

Chen K., Guo T., Li X.-M., Zhang Y.-M., Yang Y.-B., Ye W.-W., Dong N.-Q., Shi C.-L., Kan Y., Xiang Y.-H., Zhang H., Li Y.-C., Gao J.-P., Huang X., Zhao Q., Han B., Shan J.-X., and Lin H.-X. (2019). Translational Regulation of Plant Response to High Temperature by a Dual-Function tRNA^{His} Guanylyltransferase in Rice. Mol. Plant. **12**, 1123–1142.

INTRODUCTION

Global warming currently poses one of the most severe challenges to improving crop yields around the world. Rice (*Oryza sativa*) grows over a wide range of climatic conditions, and contributes to the food supply for >50% of the world population (Sasaki and Burr, 2000). To survive in increasingly stressful conditions, plants have evolved numerous intrinsic tolerance strategies to adapt to environmental changes (Bita and Gerats, 2013). Genetic and genomic evidence suggests that various proteins contribute to plant heat responses at different levels (Jaya et al., 2009; Kumar and Wigge, 2010; Cortijo et al., 2017). Furthermore, RNA plays important roles in the heat response in plants (Wang and Chekanova, 2016). Notably, it has been previously reported that tRNA (transfer RNA) modifications participate in the regulation of multiple biological processes

Published by the Molecular Plant Shanghai Editorial Office in association with Cell Press, an imprint of Elsevier Inc., on behalf of CSPB and IPPE, SIBS, CAS.

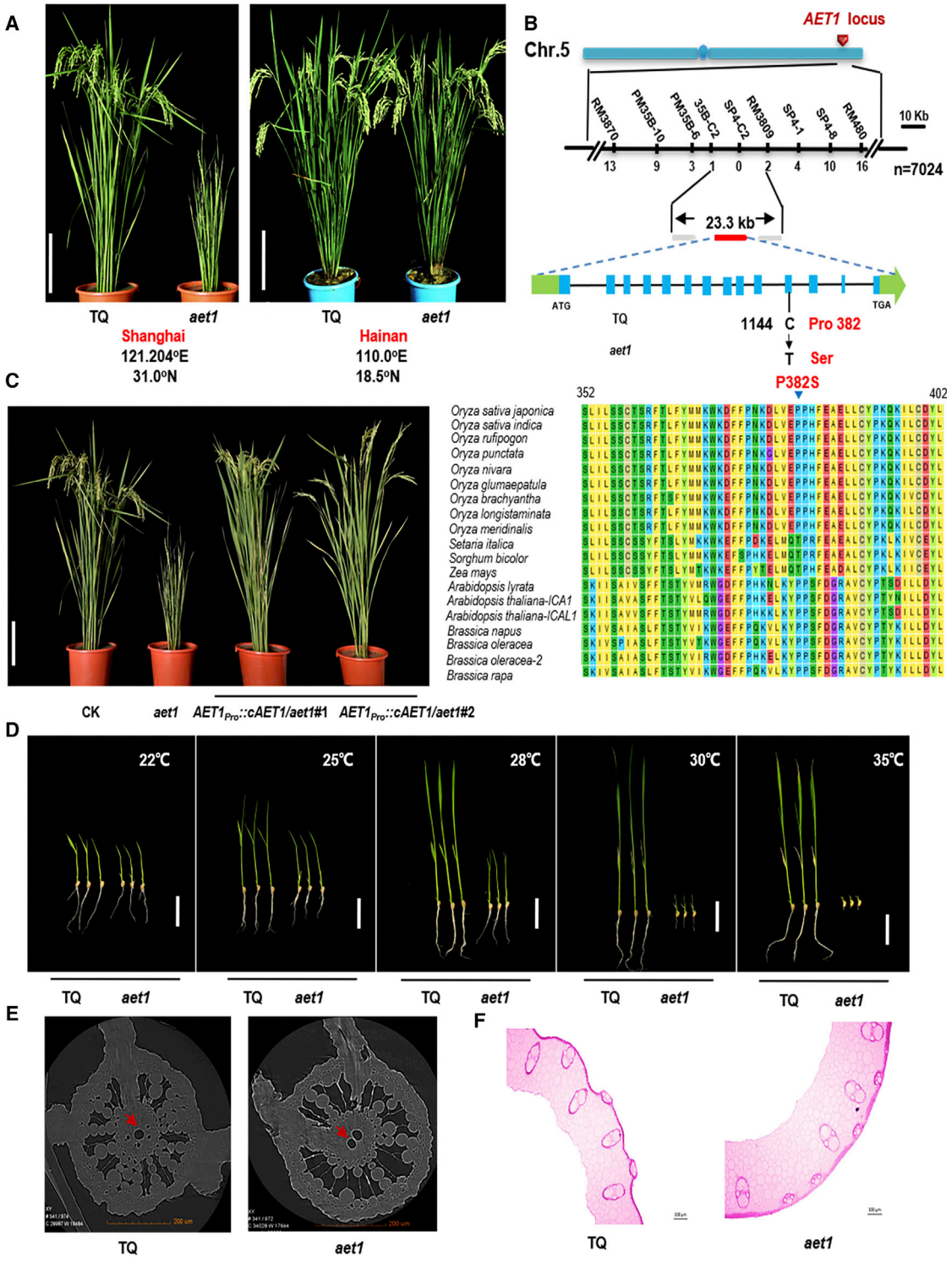

Figure 1. The *aet1* Mutant Is Thermosensitive.

(A) Plant architecture of the wild-type TQ and *aet1* mutant plants at the reproductive stage grown at two different latitudes, in Shanghai and Hainan, China. Scale bars, 20 cm.

(B) Map-based cloning of *AET1*. The *AET1* locus was initially mapped to the long arm of chromosome 5 between the marker loci RM3870 and RM480, then narrowed to a 23.3-kb region containing three genes. The numbers of recombinant individuals are shown beneath the marker locus positions. A single nucleotide mutation from C to T leads to the change of a proline to serine in the predicted AET1 protein (upper panel). An amino acid sequence alignment of partial AET1-like peptide sequences from monocots and dicots is shown. Identical and similar residues are shown in the same color; a triangle indicates the position of P382S, a proline residue that is highly conserved in multiple monocots and dicots (lower panel).

(legend continued on next page)

in plants, and the enzymes involved in tRNA processing and modification have also been shown to regulate plant development and contribute to abiotic stress response in *Arabidopsis* and rice (Chen et al., 2010; Zhou et al., 2013; Zhu et al., 2015; Wang et al., 2016, 2017a, 2017b; Jin et al., 2018). Thus, the hidden associations between tRNA modification and translational control are emerging.

In plants, ribosomes are composed of two subunits, which are assembled from four kinds of rRNA (ribosomal RNA) and 70–80 ribosomal proteins (Hinnebusch and Lorsch, 2012). Translation consists of three main steps: initiation, elongation, and termination. The initiation phase is the decisive step in translational control and has been very well studied (Merchante et al., 2017). eIF3 (eukaryote initiation factor 3) is a large, multisubunit protein complex that functions in 40S recruitment, translation initiation scanning, ternary complex formation, and other processes that contribute to protein translation initiation (Hinnebusch, 2014; Browning and Bailey-Serres, 2015). Recent studies have revealed that eIF3 functions as a translational activator by directly binding to the 5′ untranslated regions (UTRs) of specific mRNAs in animal systems (Thakor et al., 2017; Gomes-Duarte et al., 2018). Some mRNAs with 5′ UTRs that contain short open reading frame (ORF) structures are considered to have uORFs (upstream ORFs). When the translation termination phase is followed by a second initiation event at a site downstream of the uORF stop codon, the initiation phase is called translation reinitiation (Gunisova et al., 2018). eIF3h, the h subunit of eIF3, is required for translation reinitiation of uORF-containing mRNAs (Kim et al., 2004; Roy et al., 2010; Zhou et al., 2010; Zhu et al., 2015). Additionally, the scaffold protein RACK1 (receptor for activated C-kinase 1), located at the back of the head of the 40S subunit of eukaryotic ribosomes, interacts with the PCI domain of eIF3c and serves as a linking bridge between eIF3 and the 40S ribosome, which promotes translation pre-initiation (Kouba et al., 2012; Hinnebusch, 2014; Nielsen et al., 2017; Xie et al., 2018).

High temperature is a major abiotic stress in plants that has been discovered to be associated with translational control (Xu et al., 2011; Ueda et al., 2012; Zhang et al., 2017). The phytohormone auxin plays a fundamental role in plant growth in response to high temperatures, and auxin signaling has been well studied at the transcriptional level (Wigge, 2013). Recently, new evidence has emerged concerning translational control in auxin signaling (Schepetilnikov and Ryabova, 2017). Some ribosomal protein mutants repress the translation of auxin response factor (ARF) transcription factors; the translational control of ARFs involves uORFs and is necessary for the proper regulation of auxin-mediated developmental programs (Rosado et al., 2012). Furthermore, eIF3h is phosphorylated by the target of rapamycin (TOR) signaling pathway in response to auxin to promote translation reinitiation in *Arabidopsis* (Schepetilnikov et al., 2013), providing a mechanism for the positive regulation of the translation of uORF-containing mRNAs by auxin via TOR signaling activation (Schepetilnikov and Ryabova, 2018). To understand more precisely how plants sense and adapt to environmental changes, we screened a rice ethyl methanesulfonate (EMS) mutant library grown in two geographical areas with distinctly different temperature ranges to identify environmentally sensitive phenotypes. Here we report the characterization of *AET1* (*Adaptation to Environmental Temperature 1*), a gene that encodes a $tRNA^{His}$ guanylyltransferase, an enzyme that adds a guanine to the 5′ end of pre-$tRNA^{His}$ to activate $tRNA^{His}$ aminoacylation. AET1 interacts with both the RACK1A and eIF3h proteins and regulates the translational efficiency of uORF-containing mRNAs in rice. In particular, AET1 binds directly to *OsARF* mRNAs, especially the uORFs of *OsARF19* and *OsARF23*, and participates in auxin signaling in response to high temperatures. Our findings suggest that a tRNA modification enzyme has dual functions in rice: regulating the tRNA redundancy and the translational efficiency of specific mRNAs. Phylogenetic analysis shows that the frequency of haplotypic SNPs in *AET1* decreases with increasing latitude for both cultivated and wild rice varieties, suggesting that selection at the rice *AET1* locus is associated with environmental temperature.

RESULTS

Characterization of the Rice Thermosensitive Mutant *aet1*

To investigate how rice senses changes in the environment, we performed an EMS mutagenesis screen with the *indica* rice variety TQ ("TeQing") and isolated a thermosensitive mutant, which we named *aet1*. This mutant displayed distinct phenotypes when grown in Shanghai and Hainan (Figure 1A). When grown in Shanghai during a hot summer, which is considered to be a severely high-temperature condition for rice, *aet1* mutant plants displayed dwarfism with curled, narrow leaf blades, and failed to produce any seeds (Figure 1A; Supplemental Figure 1A and 1B). By contrast, in the cool winter-spring climate of Hainan, *aet1* plants showed only a slight difference in growth compared with TQ plants (Figure 1A; Supplemental Figure 1C and 1D). The *AET1* gene was isolated via a map-based cloning strategy, and a comparison of the gene sequences between wild-type TQ and *aet1* showed that a single C-to-T nucleotide transition at position 1144 in the *AET1* ORF causes a predicted amino acid change from proline to serine at position 382 (Figure 1B). The *AET1* gene is predicted to encode a $tRNA^{His}$ guanylyltransferase. Protein sequence alignments showed that the amino acid at position 382 is conserved in most dicots and monocots, and phylogenetic analysis showed that this gene is conserved in eukaryotes, including mammals (Figure 1B and Supplemental Figure 2).

To determine whether the candidate gene is responsible for the observed mutant phenotype, we performed a genetic

(C) Comparisons of plant architecture between TQ, *aet1*, and the T_2-generation complementation transgenic lines $AET1_{Pro}$::c*AET1*#1 and $AET1_{Pro}$::c*AET1*#2 that harbor the *AET1* promoter-cDNA fusion construct in the mutant *aet1* background. Scale bar, 10 cm.
(D) The phenotypes of TQ and *aet1* seedlings grown at five different temperatures for 10 days after germination. Scale bars, 5 cm.
(E) X-ray scanning images of TQ and *aet1* mutant seedling root cross sections using the Xradia 510versa 3D X-ray microscope. Arrows show that the internal structure is profoundly different between TQ and *aet1* seedlings grown at 25°C for 10 days after germination. Scale bar, 200 μm.
(F) Cross-section micrographs of TQ and *aet1* culms stained with safranin. Scale bar, 100 μm.

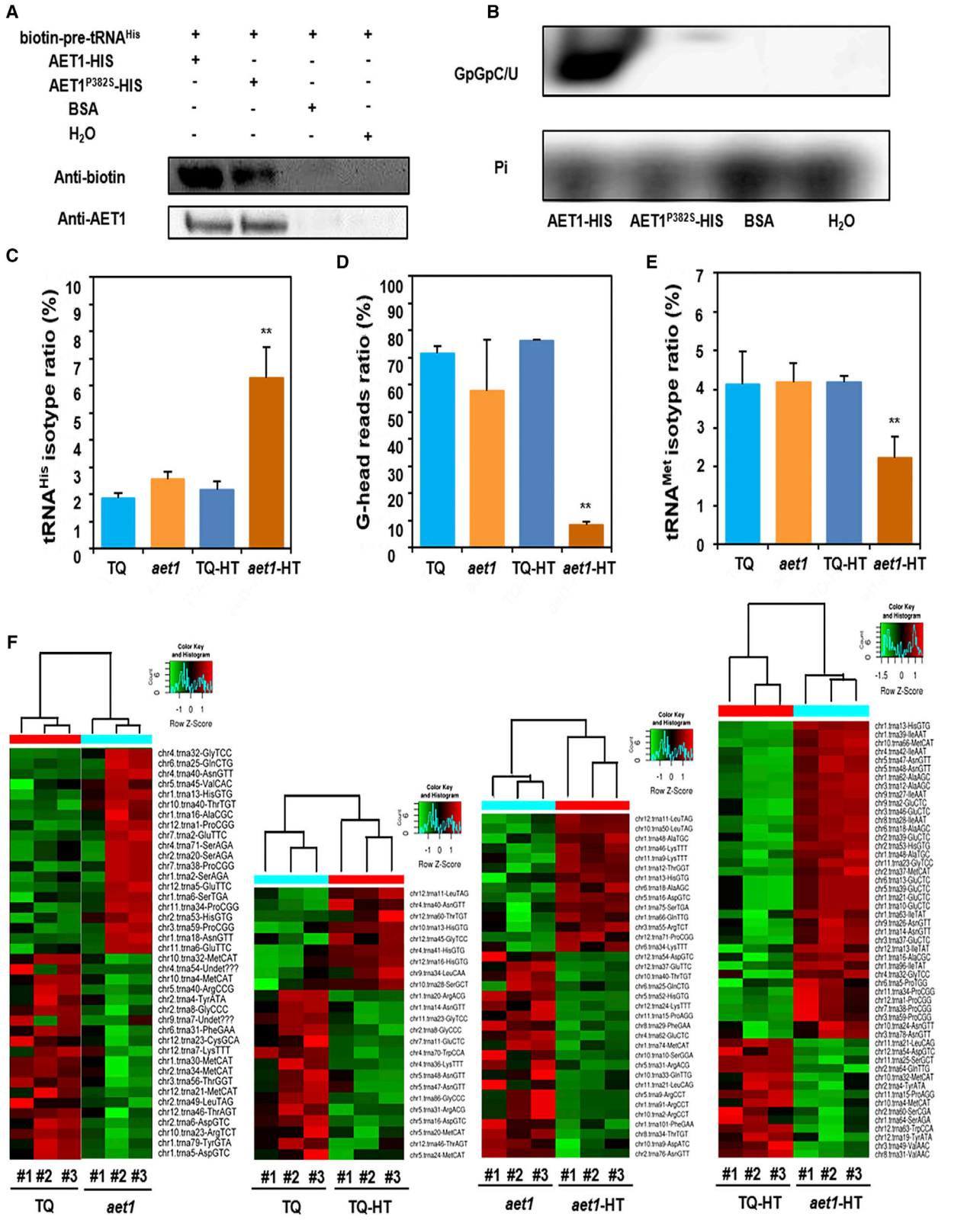

Figure 2. The *aet1* Mutation Abolishes the Guanylyltransferase Activity of AET1 *In Vitro* and Disrupts the tRNA Profile *In Vivo*.

(A) tRNA EMSA shows that AET1 and AET1^{P382S} can bind pre-tRNA^{His} *in vitro*. AET1-HIS, AET1 recombinant protein fused with the His-tag purified from *E. coli*. AET1^{P382S}-HIS, AET1 recombinant protein mutated at position 382 (proline to serine) fused with the His-tag purified from *E. coli*. We synthesized

(legend continued on next page)

complementation test and found that the transgenic complementation lines rescued the growth defects of the *aet1* plants grown in Shanghai (Figure 1C). In addition, we performed genome editing of *AET1* in the wild-type background using the CRISPR/Cas9 system and subsequently observed distinct growth defects in the positive T_2 transgenic lines grown in Shanghai (Supplemental Figure 3A and 3B). We also constructed overexpression constructs and transformed them into the mutant lines; these constructs rescued the growth defects of *aet1* plants grown in Shanghai (Supplemental Figure 4A–4D). These results showed conclusively that the mutation in *AET1* contributes to the phenotypes of the *aet1* plants grown in Shanghai. Considering that the differences between Hainan and Shanghai are mainly in temperature and photoperiod, we hypothesized that either light or temperature could cause the observed growth changes. However, we found that light is not the main factor causing the *aet1* phenotypes (Supplemental Figure 5A). When subjected to different temperatures, *aet1* seedlings displayed severe growth defects compared with TQ seedlings at high temperatures, indicating that temperature is the main factor contributing to the *aet1* growth arrest phenotype observed in Shanghai (Figure 1D and Supplemental Figure 5B). Although the growth differences between TQ and *aet1* seedlings at 25°C were obvious by 10 days after germination (Figure 1D), the *aet1* growth defects recovered under the same temperature after another 5 days of growth (Supplemental Figure 5C). Consistent with the phenotypes of the *aet1* mutant, the CRISPR/Cas9 transgenic lines were more sensitive to high temperature, but the *AET1* overexpression lines were not (Supplemental Figure 6). The *aet1* mutant was also found to be sensitive to salt and drought treatment, suggesting that *AET1* is required for normal growth in response to abiotic stress in rice (Supplemental Figure 5D and 5E).

We next used X-ray microscopy to scan the seedlings grown at 25°C, and observed that the structure of the leptocentric vascular bundle in the shoot and root of the *aet1* mutant was severely altered (Figure 1E and Supplemental Figure 7A). This result indicates that although TQ and *aet1* seedlings showed no obvious morphological differences, the ultrastructures of their tissues are very different. Microscopic examination of stem cross-sections showed that *aet1* mutant culms had smaller areas and diameters, fewer vascular bundles, and larger differences between the internal and external stems compared with the wild type, indicating that *AET1* is required for normal cell proliferation at high temperatures in Shanghai (Figure 1F and Supplemental Figure 7B–7E). Taken together, our results show that *AET1* plays important roles in rice growth and development in response to high temperature.

AET1 Is Required for tRNA^{His} Maturation and tRNA Homeostasis

The *AET1* gene encodes a tRNA^{His} guanylyltransferase containing two repeated Thg1 domains and two repeated Thg1C domains. The *Thg1* gene in yeast has been well characterized and shown to belong to a unique enzyme family, members of which contain 3′-to-5′ RNA/DNA polymerase activity (Jackman and Phizicky, 2006). Recent research has revealed that ICA1 in *Arabidopsis* sharing 49.81% protein similarity with AET1, has similar effects in response to high temperature (Zhu et al., 2015). To determine whether AET1 has tRNA^{His} binding ability, we conducted a tRNA electrophoretic mobility shift assay (EMSA) and found that both AET1-HIS and AET1^{P382S}-HIS bind to pre-tRNA^{His} (Figure 2A). Using *in vitro* enzyme assays (Jackman and Phizicky, 2006), we confirmed that AET1-HIS has catalytic activity and adds a guanine to the 5′ end of pre-tRNA^{His}, while AET1^{P382S}-HIS has almost no catalytic activity (Figure 2B), implying that the proline at position 382 is essential for tRNA^{His} guanylyltransferase activity.

We then used tRNA sequencing (Pang et al., 2014; Zheng et al., 2015) to explore the fluctuations in mature tRNA levels in TQ and *aet1* plants under normal- and high-temperature conditions. The tRNA-sequencing results showed that total tRNA^{His} isotype levels in *aet1* plants are slightly higher than those in TQ plants at normal temperature, but are much higher in *aet1* than in TQ under high-temperature conditions, indicating that *aet1* plants need to acquire more tRNA^{His} to compensate for the functional loss of *aet1* and that elevated temperature accelerates this process (Figure 2C). We next examined the percentage of tRNA^{His} reads with (G-head) and without (non-G-head) a 5’ guanosine and discovered that the ratio of tRNA^{His} G-head reads to all tRNA^{His} reads in TQ remained almost the same across temperature treatments, while the tRNA^{His} G-head reads ratio in *aet1* plants dramatically decreased in response to high-temperature treatment (Figure 2D). These results suggest that a certain degree of enzyme activity is present in *aet1* plants grown at normal temperature, while enzyme activity is lost under high-temperature conditions. We also analyzed the reads for tRNA^{Ala} and tRNA^{Trp} isotypes and found no reads with an extra 5’ guanosine in these isoptypes, indicating that the G-addition reaction is specific for tRNA^{His}, which confirms previous *in vivo* research (Jackman and Phizicky, 2006) (Supplemental Table 1).

biotin-linked pre-tRNAHis and incubated it with the recombinant proteins for 2 h, ran the assays on a native polyacrylamide gel, and used anti-biotin and anti-AET1 antibodies to detect the protein bands.

(B) Thg1 enzyme assay indicates that AET1 possesses 3′-to-5′ reverse polymerase activity, and AET1^{P382S} fails to add G_{-1} to tRNA^{His} *in vitro*. Pre-tRNA^{His} was labeled with [γ-^{32}P]ATP and incubated with the samples for 1 h, and RNase A and calf intestinal alkaline phosphatase were used to digest the tRNA fragments. The AET1 protein can add a guanine to the 5′ end of pre-tRNA^{His}, resulting in GpGpC fragments that diffuse on TLC plates, but the mutant AET1^{P382S} protein fails to add a guanine to the 5′ end, leading to an absence of GpGpC fragments.

(C–E) Comparisons of the tRNA^{His} isotype ratio (**C**), the ratio of tRNA^{His} G-head reads to all tRNA^{His} reads (**D**), and the tRNA^{Met} isotype ratio (**E**) in TQ, *aet1*, TQ-HT, and *aet1*-HT determined from tRNA-seq data. HT refers to high-temperature treatment. Each tRNA is encoded by multiple genes with the same function, which together act as common tRNA isotypes. The G-head ratio was calculated by dividing the number of G-head reads (the number of tRNA^{His} transcripts with a 5′ guanosines) divided by the number of all transcripts (number of all the sequenced 5′ tRNA^{His} transcripts). Values are given as the mean ± standard deviation. $^{*}P < 0.05$; $^{**}P < 0.01$ compared with the corresponding TQ control using Student’s *t*-test.

(F) Clustering heatmaps of tRNA differential expression patterns in TQ, *aet1*, TQ-HT, and *aet1*-HT plants derived from tRNA-sequencing data. Standard scores (*Z*-scores) were used as the numerical signs to evaluate the standard deviations from the mean of the corresponding samples.

A previous study has shown that $tRNA^{Met}$ is important for the initiation of protein synthesis, and that its abundance contributes to translational efficiency (Hinnebusch and Lorsch, 2012). We also observed that the $tRNA^{Met}$ isotype ratio in *aet1* plants grown at 35°C was markedly reduced to only half the level in TQ plants, indicating that the rate of protein synthesis in the mutant decreased in response to high-temperature treatment (Figure 2E). These results imply that the enhanced growth defects observed in the mutant plants grown at high temperature are associated with the diminished level of $tRNA^{Met}$. In addition to $tRNA^{Met}$, the isotype ratios for other tRNAs also differed between TQ and *aet1* plants, especially in response to high temperature, which reshapes tRNA profiles, implying that *AET1* is essential for maintenance of tRNA abundance (Supplemental Figure 8). A previous study showed that tRNA abundance is a key factor that affects translational efficiency (Lian et al., 2016). We next explored the tRNA distribution in TQ, *aet1*, TQ-HT, and *aet1*-HT plants (HT refers to high-temperature treatment), and found that mutating *AET1* contributed more to the disruption of tRNA profiles than high temperature (Figure 2F). Taken together, our study confirmed that AET1 has $tRNA^{His}$ guanylyltransferase activity, and that this activity is required for $tRNA^{His}$ maturation in rice. The tRNA-sequencing data showed that AET1-mediated tRNA modification contributes to the global tRNA abundance and is associated with translational efficiency in response to high temperature.

AET1 Interacts with Both RACK1A and eIF3h in the Endoplasmic Reticulum

To explore the molecular mechanism by which AET1 regulates plant development in response to high temperature, we used the yeast two-hybrid system to screen for proteins that interact physically with AET1. Interestingly, the ribosome-associated proteins RACK1A and eIF3h both interact with AET1. Moreover, we found that AET1, RACK1A, and eIF3h can interact with each other (Figure 3A). In addition, *in vitro* pull-down assays also confirmed that His-tagged AET1 is able to pull down maltose binding protein (MBP)-tagged RACK1A and eIF3h (Supplemental Figure 9A). We also constructed glutathione *S*-transferase (GST)-tagged RACK1A, and the fusion protein was able to pull down MBP-tagged eIF3h as well (Supplemental Figure 9B). These results confirm that the three proteins interact with each other. We also used biomolecular fluorescence complementation (BiFC) assays and observed that the RACK1A-nYFP fusion protein interacted with eIF3h-cYFP and AET1-cYFP, and that RACK1A-cYFP interacted with eIF3h-nYFP and AET1-nYFP. AET1-nYFP could also interact with eIF3h-cYFP and vice versa (Figure 3B and Supplemental Figure 10A). These results confirm that AET1 interacts with both RACK1A and eIF3h *in vivo*.

To further determine where the three interacting proteins function *in vivo*, we constructed PA7-AET1-YFP, PA7-eIF3h-YFP, and PA7-RACK1A-YFP fusions, and separately transformed them into rice protoplast cells. Fluorescent signals from each of the three protein fusions and the ribosome protein S2 protein fusion overlapped exactly with endoplasmic reticulum (ER)-marker protein fluorescence (Nelson et al., 2007), indicating that they all function in the ER and are associated with the ribosome (Figure 3C and Supplemental Figure 10B). We further found that the three interacting proteins colocalized with the AAPT2 (AT3G25585) protein, which has been proposed to localize to the ER (Liu et al., 2015), suggesting that AET1 interacts with both RACK1A and eIF3h in the ER (Supplemental Figure 11). We assayed the expression patterns of *AET1*, *RACK1A*, and *eIF3h* using qRT–PCR and β-glucuronidase (GUS) staining, and found that they are expressed in almost all tissues, which is consistent with their functions in general protein synthesis (Supplemental Figure 12). Taken together, these results strongly imply that AET1 interacts with both RACK1A and eIF3h in the ER, and is associated with translational regulation.

AET1, but not RACK1A and eIF3h, Can Directly Bind *OsARF* mRNAs

Given that AET1 interacts with both RACK1A and eIF3h, which are involved in translation, we asked whether the interacting proteins can associate with mRNAs. We thus performed RNA immunoprecipitation sequencing (RIP-seq) to identify mRNAs that co-immunoprecipitate with AET1. The RIP-seq results revealed that AET1 can recognize 545 unique mRNAs in the wild-type TQ, but only 208 unique mRNAs in *aet1* mutant plants under high temperature; 50 of the genes were found to be common to both samples (Supplemental Figure 13A). KEGG (Kyoto Encyclopedia of Genes and Genomes) pathway analysis indicated that endogenous AET1 mainly interacts with mRNAs for genes that belong to photosynthetic processes and metabolism-related processes in TQ-HT plants, and with mRNAs for genes that are involved in amino acid metabolism pathways in *aet1*-HT plants (Supplemental Figure 13B). These results suggest that the loss of function of AET1 may affect protein synthesis through imbalances in tRNA distribution. Strikingly, a heatmap revealed that there is an obvious difference in enriched auxin-associated genes between TQ and *aet1* at high temperature, in which the *OsARF* genes were dramatically enriched (Supplemental Figure 13C). These results imply that *AET1* may modulate auxin signaling by regulating the *OsARFs* in response to high temperature.

To confirm the RIP-seq results, we performed RIP–qRT–PCR assays with AET1 using mRNA isolated from TQ-HT and *aet1*-HT plants. We found that the uORF and main ORF (mORF) of *OsARF19* were enriched after immunoprecipitation, but the negative control *OsActin* was not immunoprecipitated, and that the relative enrichment of the *OsARF19* uORF and mORF differed between TQ-HT and *aet1*-HT (Figure 4A, 4B, and 4E). In addition, *OsARF23* and *OsARF2* were also found to be precipitated by AET1 in both the wild type and mutant samples (Figure 4C and 4D). Based on a previous study showing that several *OsARF* mRNAs contain uORFs that hinder eIF3h-dependent translation in *Arabidopsis* (Zhou et al., 2010), we inferred that the uORFs of *OsARFs* suppress the translation of the mORFs. We thus predicted the uORF structures of the 25 *OsARFs* in rice and found that 17 *OsARFs* had potential uORF structures (Supplemental Figure 14). It is worth noting that *OsARF19* is predicted to contain two potential uORFs, and the first uORF - as well as the mORF of *OsARF19* were detected by RIP-qRT–PCR (Figure 4A and 4B; Supplemental Figure 14). In addition, the *OsARF23* mRNA has also been found to contain the specific "start–stop" uORF structure (Supplemental Figure 14) (Gunisova

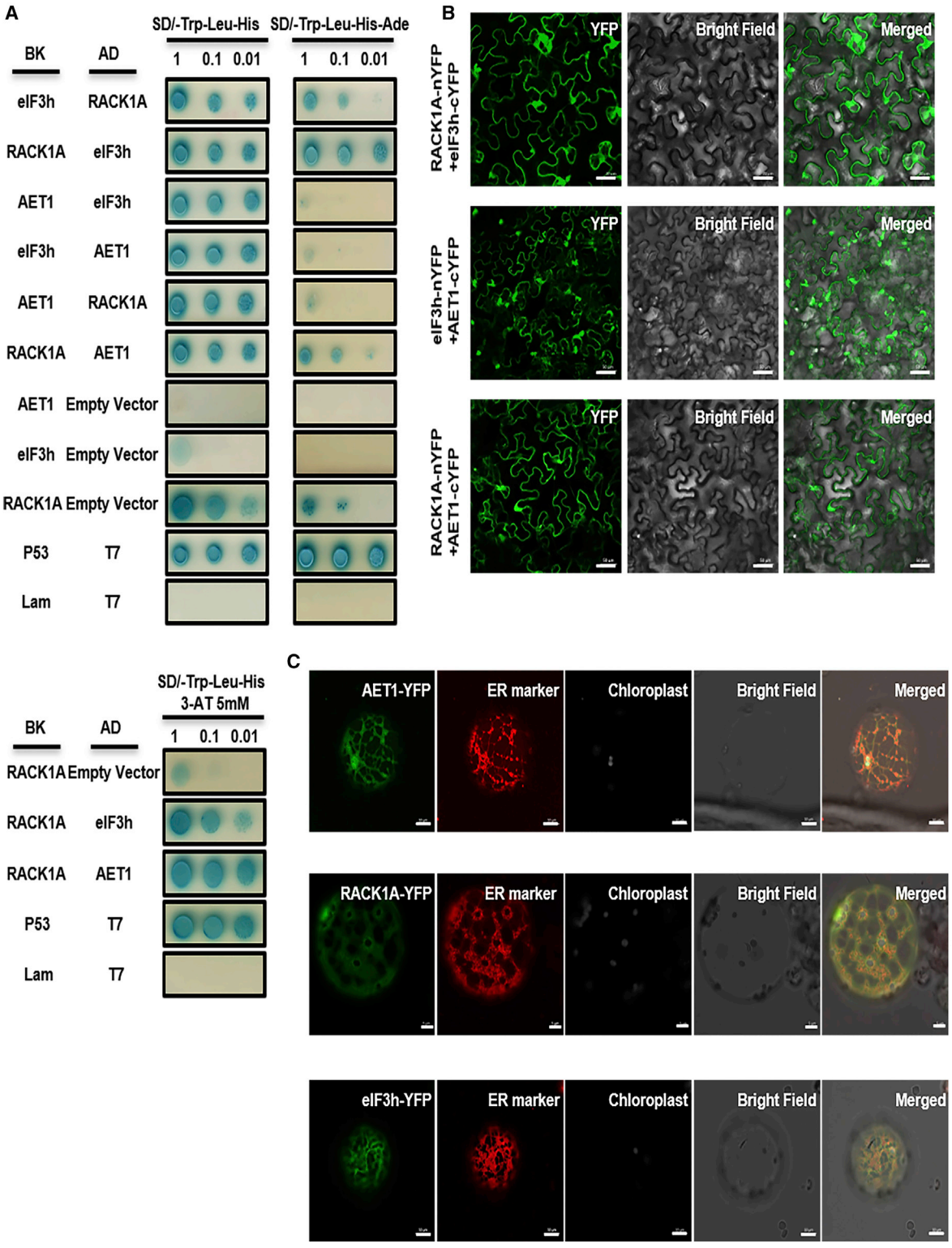

Figure 3. AET1 Interacts with Both RACK1A and eIF3h in the ER.

(A) Yeast two-hybrid assays indicate that AET1 interacts with both RACK1A and eIF3h. Most of the yeast colonies could be grown on SD/-Trp-Leu-His medium, yet the interactions are weak since no obvious growth could be seen on SD/-Trp-Leu-His-Ade medium. RACK1A self-activation could be inhibited by adding 5 mM 3-AT to the SD/-Trp-Leu-His medium.

(B) BiFC assays show that AET1, RACK1A, and eIF3h associate with each other in *N. benthamiana* leaf cells. The genes were fused to *nYFP* (N-terminal fragment of the YFP gene) and *cYFP* (C-terminal fragment of the YFP gene) individually and co-expressed in *N. benthamiana* leaves via agroinfiltration. Scale bars, 50 μm.

(C) Subcellular co-localization of the AET1-YFP, RACK1A-YFP, and eIF3h-YFP protein fusions with an ER marker in rice protoplasts. Scale bars, 10 μm.

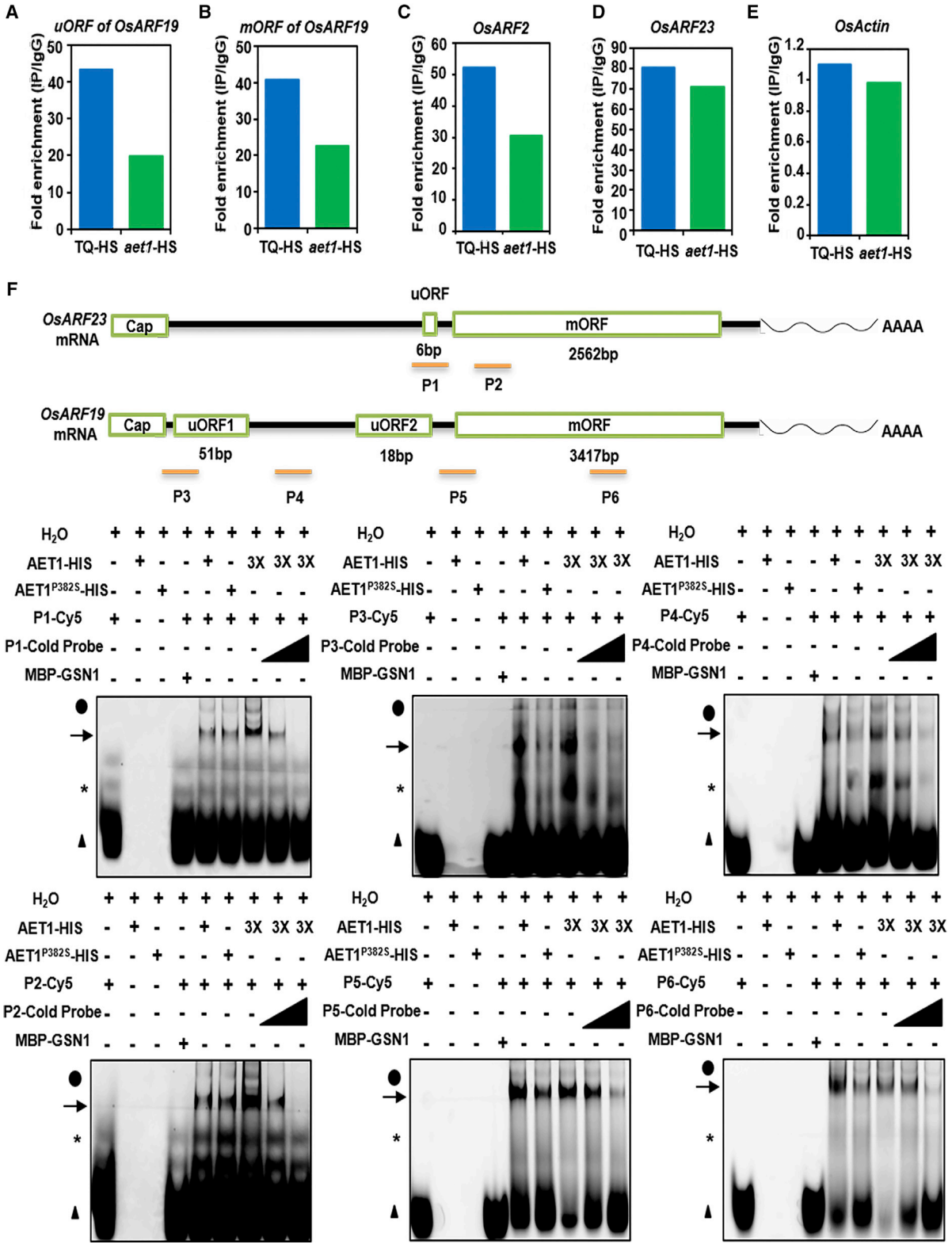

Figure 4. AET1 Directly Binds to Auxin Response Factor mRNAs.

(A–E) RNA immunoprecipitation assays confirm that AET1 is able to bind *OsARF* mRNAs *in vivo*. We used qRT–PCR to calculate the fold enrichment of the *OsARF19* uORF **(A)**, the *OsARF19* mORF **(B)**, *OsARF2* **(C)**, *OsARF23* **(D)**, and *OsActin* **(E)**.

(F) REMSA shows that AET1 can directly bind to various regions of the *OsARF19* and *OsARF23* mRNAs *in vitro*. Six probes labeled with Cy5 were designed to detect the binding of AET1 to the mRNAs. MBP-GSN1 was used as the negative control. The dots, arrows, asterisks, and triangles indicate the dimer upshifted bands, the upshifted bands, non-specific binding, and free probe, respectively.

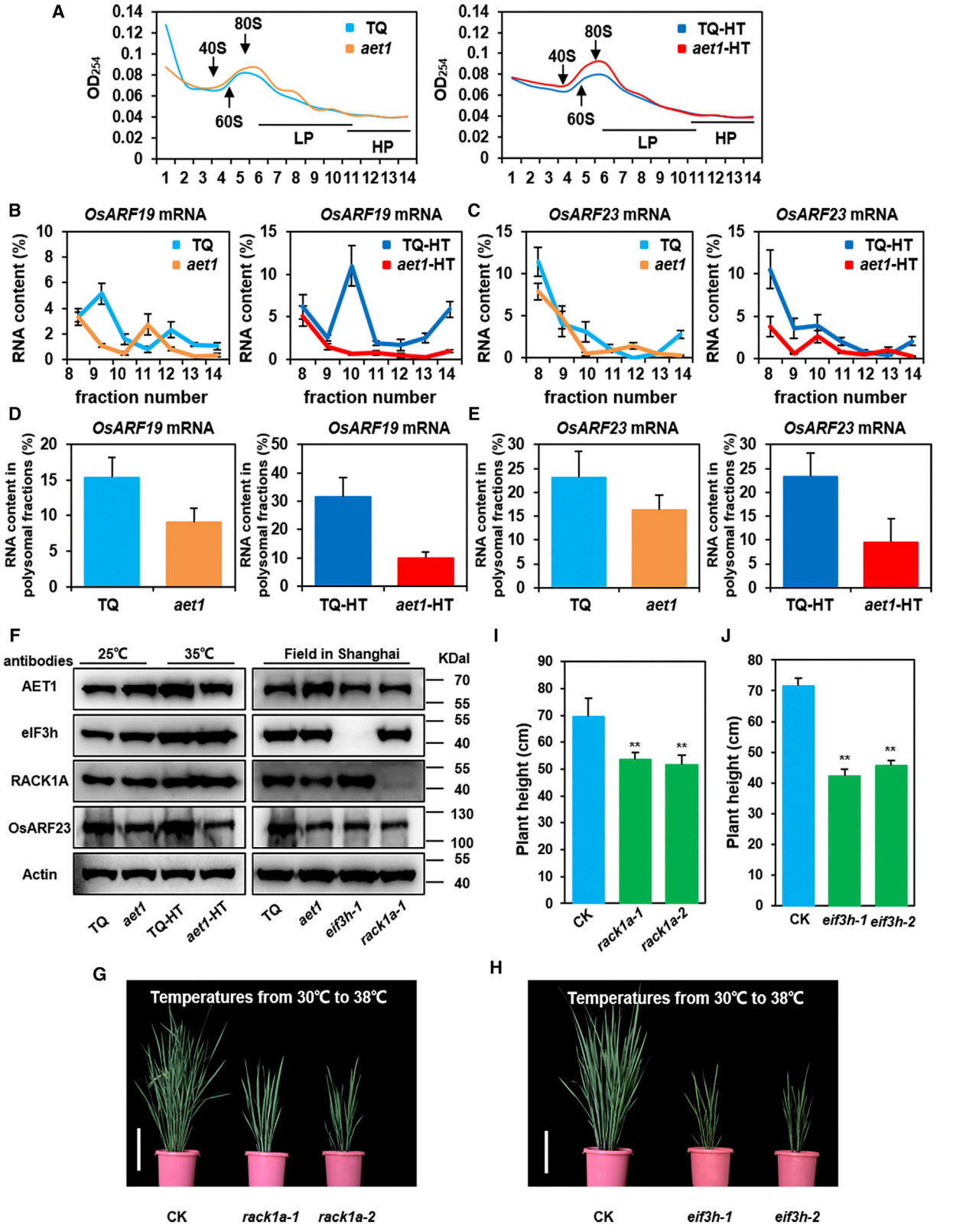

Figure 5. AET1, Together with RACK1A and eIF3h, Regulates Translational Efficiency of *OsARF* mRNAs.

(A) 20%–60% sucrose gradient absorbance (OD_{254}) profiles of ribosome complexes obtained from wild-type TQ and *aet1* mutant seedlings grown at 25°C (normal temperature) for 14 days, and at 25°C for 7 days then transferred to 35°C for 7 days (high temperature, HT). LP refers to light polysomes, HP to heavy polysomes.

(legend continued on next page)

et al., 2018). These results suggest that AET1 can associate with *OsARF* mRNAs to regulate auxin signaling at high temperature.

To better understand the details of how AET1 binds to mRNAs, we designed six Cy5 end-labeled RNA probes for different regions of Os*ARF19* and *OsARF23* covering their uORFs and mORFs, and used RNA EMSA (REMSA) to detect the binding of AET1 to the *OsARF19* and *OsARF23* mRNAs. The results showed that the AET1-HIS and AET1^{P382S}-HIS fusion proteins can both bind to the six probes individually, but that the non-ribosome-associated protein GSN1 (Guo et al., 2018) cannot, supporting the notion that AET1 directly binds to *OsARF19* and *OsARF23* mRNAs, and that the mutation in AET1^{P382S} does not affect its affinity for these mRNAs (Figure 4F). We then determined whether eIF3h and RACK1A also have affinity for mRNAs. Interestingly, we observed that neither the eIF3h nor RACK1A fusion protein could bind to the *OsARF19* and *OsARF23* mRNA probes (Supplemental Figure 15), and that the eIF3h and RACK1A fusion proteins did not affect the ability of AET1 to shift the mRNA probe signals (Supplemental Figure 16A). We also observed that AET1 could bind to the non-uORF-containing *HSF1A* and *HSF2A* mRNAs, suggesting that the binding of AET1 to mRNAs may be non-specific (Supplemental Figure 16B). With these results, we conclude that AET1, but not RACK1A and eIF3h, binds to *OsARF* mRNAs without specificity, which contributes to the regulation of *OsARF* mRNA translation.

AET1 Associates with RACK1A and eIF3h to Regulate the Translational Efficiency of *OsARF* mRNAs

RACK1 is well known to locate to the 40S ribosomal subunit, and eIF3h is a subunit of the eIF3 complex that associates with ribosomes (Kim et al., 2007; Nielsen et al., 2017). However, the molecular basis of the association of AET1 with RACK1A and eIF3h, and how it contributes to translational control, is unknown in rice. Using the polysome profiling strategy, we compared the OD_{254} of gradient fractions from TQ and *aet1* mutant plants under normal- and high-temperature conditions. OD_{254} measurements of the wild-type and *aet1* extracts showed that the 40S ribosomal subunit, 60S ribosomal subunit, and 80S monosome fractions together with the polysomal fractions are almost identical at normal temperature (Figure 5A). Consistent with this, the polysome status in TQ and *aet1* plants remained similar under high-temperature conditions.

We next examined the relative levels of the mRNAs of *OsARF19* and *OsARF23* in the polysomal fractions in TQ and *aet1* plants under both normal and high temperatures. We extracted RNAs from fractions 8 to 14 and performed qRT–PCR to measure the RNA levels of these genes; luciferase RNA was added to each fraction to normalize the data. The results showed that the *OsARF19* mRNA content in *aet1* was slightly lower than that in TQ in most of the polysomal fractions except for fraction 11 (Figure 5B, left), while in high temperature conditions, the *OsARF19* mRNA content in *aet1*-HT was significantly reduced in fractions 10 and 14 (Figure 5B, right). Under the normal temperature, the *OsARF23* mRNA content in *aet1* was lower than that in TQ in fractions 8, 10, and 14 (Figure 5C, left). At the high temperature, the *OsARF23* mRNA content was also lower in *aet1*-HT than in TQ-HT, especially in fractions 8, 9, 10, 11, and 14 (Figure 5C, right). We also calculated the total RNA content in all polysome fractions from TQ and *aet1* under normal and high temperatures. The results show that the total contents of *OsARF19* and *OsARF23* RNA in *aet1* are lower than those in TQ (Figure 5D and 5E). Taken together, our data suggest that the translational efficiency of *OsARF19* and *OsARF23* is reduced in *aet1* under normal- and high-temperature conditions.

To further validate these findings, we performed genome editing of *RACK1A* and *eIF3h* using the CRISPR/Cas9 system (Ma et al., 2015), and found that the knockout mutants all displayed obvious defects, including shorter plant height, a smaller tiller number, and lower fertility (Figure 5G–5J; Supplemental Figure 17A and 17B). These results indicate that *RACK1A* and *eIF3h* are also involved in regulating plant growth in rice. Moreover, we assayed the endogenous expression levels of AET1, eIF3h, RACK1A, and OsARF23 under different conditions and found that the AET1, eIF3h, and RACK1A proteins are induced by high temperature, which is consistent with the increase in

(B) Polysomal distribution of *OsARF19* transcripts in TQ and *aet1* seedlings grown under normal- and high-temperature conditions. The relative expression level of *OsARF19* in each polysomal fraction was calculated as the percentage of the amount of *OsARF19* expression to the amount of total RNA. Luciferase RNA was added to each fraction to normalize the data. Standard deviations were calculated from three biological repeats.
(C) Polysomal distribution of *OsARF23* transcripts in TQ and *aet1* seedlings grown under normal- and high-temperature conditions. The relative expression of *OsARF23* in each polysomal fraction was calculated as the percentage of the amount of *OsARF19* expression to the amount of total RNA. Luciferase RNA was added to each fraction to normalize the data. Standard deviations were calculated from three biological repeats.
(D) Total content of *OsARF19* transcripts in all polysome fractions from TQ and *aet1* seedlings grown under normal- and high-temperature conditions. Standard deviations were calculated from three biological repeats.
(E) Total content of *OsARF23* transcripts in all polysome fractions from TQ and *aet1* seedlings grown under normal- and high-temperature conditions. Standard deviations were calculated from three biological repeats.
(F) Western blot analysis of AET1, eIF3h, RACK1A, OsARF23, and Actin in total proteins extracted from TQ and *aet1* plants grown at 25°C and 35°C (left panel), and in total proteins extracted from TQ, *aet1*, *eif3h-1*, and *rack1a-1* grown under field conditions in Shanghai (right panel). The sizes of protein markers (in kDa) are shown to the right of the figure.
(G) Comparison of plant architecture between the CK (negative control in TQ background), and *rack1a-1* and *rack1a-2* knockout mutants derived from CRISPR/Cas9 mutagenesis grown in Shanghai in July. Scale bar, 15 cm.
(H) Comparison of plant architecture between the CK (negative control in TQ background), and *eif3h-1* and *eif3h-2* knockout mutants derived from CRISPR/Cas9 mutagenesis grown in Shanghai in July. Scale bar, 15 cm.
(I) Comparisons of plant height between CK, *rack1a-1*, and *rack1a-2*, $n = 10$ (plants).
(J) Comparisons of plant height between CK, *eif3h-1*, and *eif3h-2*, $n = 10$ (plants).
Values are given as the mean ± standard deviation. $^{**}P < 0.01$ compared with the negative control using Student's *t*-test **(I and J)**.

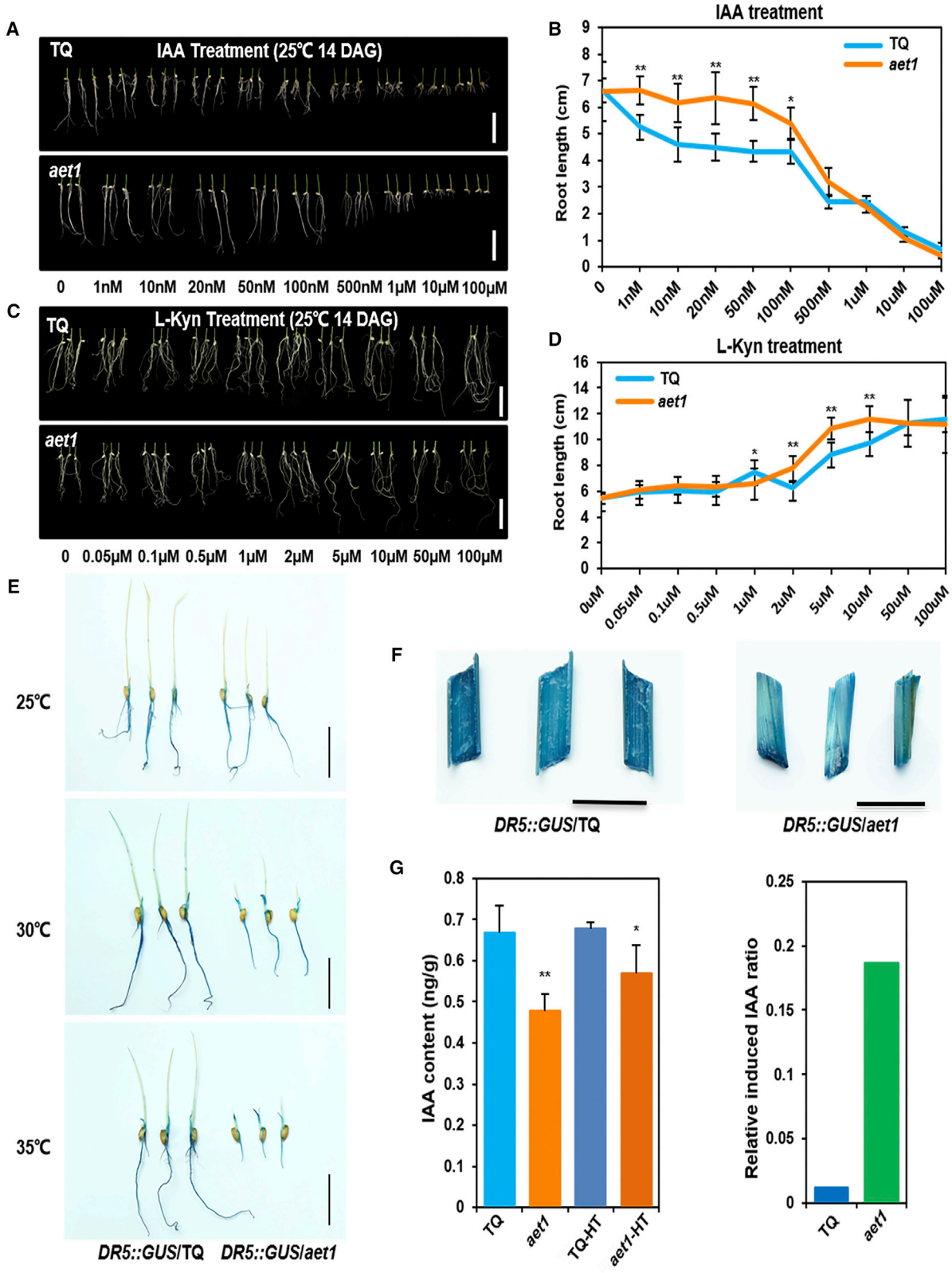

Figure 6. *aet1* Is an Auxin-Insensitive Mutant.

(A) IAA concentrations from 0 to 100 μm were used to treat seedlings of TQ and *aet1* grown at 25°C for 14 days after germination (DAG). Scale bar, 2 cm.

(B) Statistical analysis of auxin treatment of TQ and *aet1* seedlings grown under normal conditions for 10 DAG, $n = 30$ (plants). Root length values are given as the mean ± standard deviation. $^{*}P < 0.05$; $^{**}P < 0.01$ compared with the corresponding TQ control seedlings using Student's *t*-test.

(legend continued on next page)

transcription levels (Figure 5F and Supplemental Figure 18A–18C). Notably, the abundance of the OsARF23 protein was decreased in the *aet1* mutant compared with that in TQ at the normal temperature. At the high temperature, OsARF23 accumulation was induced in the wild-type TQ but obviously decreased in the *aet1* mutant, and the level of OsARF23 protein was significantly lower than that at the normal temperature (Figure 5F). These results indicate that mutation of *AET1* reduces translational efficiency of the OsARF23 protein. In accordance with this, the OsARF23 protein level was also decreased in the *RACK1A* and *eIF3h* knockout mutants (Figure 5F). These data suggest that the interaction of AET1 with RACK1A and eIF3h indeed affects the translational efficiency of *OsARFs*. Additionally, we observed the phenotypes of *OsARF23* knockout mutants under normal- and high-temperature conditions and found that the mutants are more sensitive to high temperature compared with the wild type (Supplemental Figure 17C–17I). Taken together, these results confirm that the association of AET1 with RACK1A and eIF3h regulates the translational efficiency of *OsARF* mRNAs, which modulate auxin signaling, and contributes to normal growth at high temperature.

AET1 Is Required for Normal Plant Response to Exogenous Auxin and High Temperature

Because we discovered that the three interacting proteins, AET1, RACK1, and eIF3h, can regulate translational efficiency of *OsARF* mRNAs, we asked whether mutation in *AET1* causes defective auxin signaling. We used 10 different concentrations of exogenous indole-3-acetic acid (IAA) to treat TQ and *aet1* plants grown at 25°C for 14 days after germination. Interestingly, *aet1* mutant plants were much less sensitive to IAA treatment compared with the wild type, indicating that *AET1* might be involved in the auxin signaling pathway (Figure 6A and 6B). The auxin biosynthesis inhibitor L-kynurenine (L-Kyn) was also used to treat TQ and *aet1* seedlings grown under the same conditions (He et al., 2011); we observed that the *aet1* mutant showed hypersensitivity to exogenous L-Kyn application as judged by root length (Figure 6C and 6D). These results suggest that *AET1* is required for the auxin response. Furthermore, staining for GUS activity in transgenic plants expressing the *GUS* gene driven by the auxin-responsive *DR5* promoter confirmed that auxin signaling was strongly repressed in the *aet1* mutant at high temperatures (Figure 6E and 6F). We further assayed the auxin levels in both TQ and *aet1* plants under normal- and high-temperature conditions, and found that the endogenous auxin content of *aet1* was decreased compared with TQ; however, at high temperatures the relative level of IAA in *aet1* plants dramatically increased (Figure 6G). We found that several auxin response genes were downregulated in the *aet1* mutant under high temperature (Supplemental Figure 19A and 19B). These results suggest that *AET1* is involved in the regulation of auxin signal transduction and is required for normal plant growth in response to high temperature.

To further evaluate the cell cycle in TQ and *aet1* plants, we used flow cytometry to analyze the cell-division rate in root tips. We found that the percentage of G_2/M-phase cells with higher 4C DNA content was lower in *aet1* root tips, but that the percentage of G_1-phase cells with 2C DNA content increased with a new cell-cycle distribution in response to high temperature, indicating that the mutation of *AET1* disrupts cell proliferation leading to arrested development in rice (Supplemental Figure 20A and 20B). This is supported by qRT–PCR data showing that the expression levels of some cell-cycle-related genes are clearly downregulated at the high temperature (Supplemental Figure 20C and 20D). In summary, these data suggest that *aet1* is an auxin-insensitive mutant, and that *AET1* contributes to auxin signaling associated with cell division during high temperature, implying that translational control associated with tRNA modification plays an important role in auxin signaling output under stress conditions.

We further surveyed 1083 *O. sativa* varieties and 446 *Oryza rufipogon* accessions for *AET1* haplotypes (Huang et al., 2011). We found that the frequency of several haplotypic SNPs within this group of cultivated and wild rice accessions is associated with geographical distribution. The frequency of non-reference alleles declines with decreasing climatic temperature for both the cultivated and wild rice accessions (Supplemental Figure 21A and 21B). These results indicate that the *AET1* promoter region has been under environmental selection pressure, mainly related to temperature. We then used the pan-genome data to analyze the *AET1* haplotypes in 67 rice accessions of *O. sativa* and *O. rufipogon*, and generated a phylogenetic tree from an alignment of the gene sequences from these rice accessions using MEGA 7.0 and the Interactive Tree of Life (iTOL) (Kumar et al., 2016; Letunic and Bork, 2016; Zhao et al., 2018) (Supplemental Figure 21C). The *AET1* alleles are separated into two major clades, and the tree shows that the alleles found in the modern cultivars in both clades originated from *O. rufipogon*. Taken together, the data shows that *AET1* contributes to the acclimation to environmental temperature in rice.

DISCUSSION

Understanding how plants sense and respond to environmental temperatures is crucial because of global climate change, which affects the geographical distribution of plants, and could help to increase crop yields. Recent studies have shown that various genes/pathways in plants are involved in sensing ambient temperatures and responding to higher temperatures (Wigge,

(C) Seedlings of TQ and *aet1* grown at 25°C for 14 DAG were treated with L-Kyn at concentrations ranging from 0 to 100 μm. Scale bar, 2 cm.
(D) Statistical analysis of L-Kyn treatment of TQ and *aet1* seedlings grown under normal conditions for 10 DAG, $n = 30$ (plants). Root lengths are given as the mean ± standard deviation. $^*P < 0.05$; $^{**}P < 0.01$ compared with the corresponding TQ control seedlings using Student's *t*-test.
(E) GUS staining of transgenic rice seedlings expressing *DR5*::*GUS* in the TQ and *aet1* backgrounds grown at 25°C, 30°C, and 35°C for 7 DAG.
(F) Histochemical analysis of *DR5*::*GUS* transgenic lines. Shoots from field-grown transgenic *DR5*::*GUS* plants in the TQ and *aet1* backgrounds were stained for GUS activity detection. Scale bar, 3 cm.
(G) Comparisons of endogenous auxin levels in TQ, *aet1*, TQ-HT, and *aet1*-HT seedlings (left panel), and statistical analysis of induced IAA ratios in TQ and *aet1* seedlings (right panel). Each sample had three biological replicates. Values are given as the mean ± standard deviation. $^*P < 0.05$; $^{**}P < 0.01$ compared with the corresponding TQ control seedlings using Student's *t*-test.

2013). However, the relationship between tRNA modification and translation regulation under high temperatures remains elusive. In our work, we discovered that tRNA modification by a $tRNA^{His}$ guanylyltransferase plays an essential role in translational regulation of auxin signaling in collaboration with the core components of the ribosome complex, which contributes to temperature acclimation.

Previous studies have reported the functions of the RACK1/ASC1 and eIF3c/NIP1 proteins in *Saccharomyces cerevisiae*; these studies have linked the RACK1 and eIF3 complex to the promotion of translation pre-initiation with the 40S ribosomal subunit (Sengupta et al., 2004; Kouba et al., 2012). These results indicate that yeast RACK1/ASC1 function as scaffold proteins recruiting initiation factors or other proteins to the ribosome to regulate translational efficiency. Consistent with this, we found that the homologous protein in rice, RACK1A, interacts with both eIF3h and AET1, and possibly regulates translational reinitiation of uORF-containing genes via the direct binding of AET1 to the mRNAs; *rack1a* knockout mutants displayed obvious growth defects in Shanghai, supporting the proposed role of RACK1A as a ribosomal signaling hub (Nielsen et al., 2017) (Figure 5G).

In *Arabidopsis*, ~30% of the mRNAs contain one or more uORFs in their 5′ leader sequences (Kim et al., 2007). The uORF-mediated control of translation has been demonstrated to play a vital role in plant developmental processes (Xu et al., 2017; Zhang et al., 2018). In principle, uORFs form a functional barrier to translation of a downstream cistron, and most uORFs effectively downregulate translation of the mORFs (Gunisova et al., 2018). An intact eIF3h protein is required for efficient translational initiation on 5′ leader sequences harboring multiple uORFs (Kim et al., 2007), implying that eIF3h may be involved in translation reinitiation of the uORF-containing transcripts, increasing their translational efficiency in response to specific stimuli. In yeast, eIF3c/NIP1 interacts with RNA and RACK1/ASC1 via its PCI domain and serves as an intermolecular bridge between eIF3 and the 40S ribosome head region (Kouba et al., 2012). Nevertheless, we found that neither the rice eIF3h nor the RACK1A protein was capable of binding to mRNAs (Supplemental Figure 15). Rather, the tRNA modification enzyme AET1 was found to directly bind to mRNAs, implying that AET1 may bridge the gap between the RACK1A and eIF3h proteins and mRNAs in plants (Figure 4). AET1 encodes a $tRNA^{His}$ guanylyltransferase and has unique polymerase activity in the 3′-to-5′ direction, which is required for the $tRNA^{His}$ maturation (Figure 2). Our results reveal not only the primary function of the $tRNA^{His}$ guanylyltransferase, but also the multifaceted roles that tRNA modification plays in tRNA abundance and translational control (Figure 2 and Supplemental Figure 8). Therefore, we hypothesize that the scaffold protein RACK1A recruits AET1 to bind the uORFs and depends on the recognition of eIF3h, which together act as translational enhancers. Furthermore, the binding of AET1 to mRNAs probably has a monitoring role- with the ‘‘leaky scanning’’ of eIF3h (Gunisova et al., 2018). Nevertheless, in addition to binding uORFs, AET1 was also observed to have affinity for mORFs, suggesting a general mechanism by which AET1 directly contributes more to translational control than to tRNA abundance; AET1-mediated mRNA recognition is non-specific and AET1 may play a global role in protein synthesis depending on the distinct ribosomal components. Therefore, together with other partner proteins, AET1, RACK1A, and eIF3h - optimize translational efficiency. Interestingly, we also found that the $tRNA^{His}$ guanylyltransferase protein family is conserved in eukaryotes (Supplemental Figure 2), suggesting that the proposed translational regulation by the three interacting proteins might also take place in mammals. Hence, our study not only confirms AET1 as a guanylyltransferase that modifies pre-$tRNA^{His}$, but also implies a new function of guanylyltransferases as mediators that bind mature mRNAs and contribute to protein translational control.

It has been widely thought that ambient temperature significantly affects plant growth and development. Recent advances have revealed the key players mediating ambient temperature signaling (Wigge, 2013). The phytohormone auxin is fundamental to plant growth, and auxin biosynthesis, signaling, and transport pathways are induced by high temperature, indicating that auxin contributes to temperature-triggered plant development (Franklin et al., 2011). However, the precise nature of translational control of the downstream ARFs under conditions of temperature stress has not yet been well established. Our results show that the rice *aet1* mutant is insensitive to exogenous auxin application (Figure 6A and 6B), and shows auxin-defective phenotypes that are enhanced by high temperature (Figure 6E and 6F), implying that tRNA modification plays an essential role in auxin signaling in response to high temperature. Interestingly, the *Arabidopsis eif3h* mutant shows similar auxin-related developmental defects (Zhou et al., 2010), and the *rack1* mutants are also less sensitive to auxin treatment (Chen et al., 2006). Consistent with these previous studies, the *rack1a-1* and *eif3h-1* mutants in rice also displayed similar auxin-defective phenotypes (Figure 5G and 5H). Furthermore, in our study the expression of the OsARF23 protein was largely reduced in the *aet1*, *rack1a-1*, and *eif3h-1* mutants (Figure 5F), and *OsARF23* knockout mutants showed sensitivity to high temperature (Supplemental Figure 17C–17I) (Li et al., 2014). These results imply that regulation of protein translation is required for the auxin signaling output, which contributes to the acclimation to changes in ambient temperature. It is worth noting that the *aet1* mutant also displays sensitivity to salt and drought stress (Supplemental Figure 5D and 5E), indicating that *AET1* may play an important global role in plant resistance to abiotic stress. Our results agree with a previous study showing that the *Arabidopsis rack1* mutant is sensitive to salt stress and acts as a negative regulator of abscisic acid signaling (Guo et al., 2009). Taken together, these results imply that the AET1-RACK1A-eIF3h module functions in multiple signaling processes by controlling translation under abiotic stress conditions, indicating that the regulation of translation by this module is a fundamental mechanism for regulation of growth and development in plants, and possibly even in mammals.

Taken together, we propose a working model to explain how AET1 affects the auxin signaling pathway through translational control with RACK1A and eIF3h, associated with tRNA

modification. At normal temperatures, the tRNA modification enzyme AET1 can add a guanine to the 5′ end of pre-tRNA^{His}, which is then activated and can be recognized by aaRS (aminoacyl tRNA synthetases). In addition, the AET1 protein can be recruited by RACK1A and function together with eIF3h to regulate translation through the binding of AET1 to uORF-containing mRNAs. These translated proteins contribute to plant development and maintain normal growth in wild-type rice. In the *aet1* mutant, the AET1^{P382S} mutant protein fails to add a guanosine to the 5′ end of pre-tRNA^{His}, which changes the tRNA abundance and reduces translational efficiency. Although there are changes to translational efficiency and tRNA abundance, the plants still maintain their general architecture due to the low demand for uORF-containing genes under non-stress conditions. Under high-temperature treatment, AET1 can activate pre-tRNA^{His} and stabilize tRNA homeostasis. In particular, the AET1-RACK1A-eIF3h module associates with the *OsARF19* and *OsARF23* mRNAs, which leads to increased translational efficiency of these mRNAs and contributes to plant development in response to high temperature. However, the failed activation of pre-tRNA^{His} in the *aet1* mutant leads to a dramatic reduction in the amount of aminoacyl-tRNA^{His}, which disrupts the tRNA abundance and represses ribosomal translation under high temperature. In the *aet1* mutant, the translational efficiency of the mRNAs encoding OsARFs and other proteins is reduced, which results in reduced translation of OsARFs and finally increases the growth arrest in plants experiencing high temperature (Figure 7).

Although our work reveals a novel molecular mechanism of translational regulation via tRNA modification through the interaction of AET1 with RACK1A and eIF3h, accurate translational control in response to high temperature in plants remains largely unclear. In future studies, other plant components involved in translation enhancement recruited by the AET1-RACK1A-eIF3h module will be identified. In addition, identification of new AET1-interacting partners as well as the dynamic profiling of tRNA modification and protein homeostasis will further extend our understanding of how plants adapt to the changing environment.

METHODS

Plant Materials and Growth Conditions

The *aet1* mutant was isolated from EMS-treated seeds of the popular *indica* rice (*O. sativa* ssp. *indica*) variety TQ ("TeQing"). The M_1-generation *aet1* mutant was crossed back to TQ to produce M_2 plants in an isogenic background. All plants were cultivated in experimental fields in Shanghai (from May to October) and Hainan (from November to April of the following year) under natural growth conditions.

Laboratory Growth Conditions and Treatments

Yoshida's rice seedling culture solution was used for the heat treatments and normal plant growth conditions. For IAA and L-Kyn treatments, rice seeds were plated on 0.5× Murashige and Skoog (MS) medium and imbibed at 25°C to germinate. The chemical components were diluted into 0.5× MS medium. For long-photoperiod treatment, all seeds were grown at 25°C under 16 h light and 8 h dark for 14 days. For NaCl treatment, 125 mM NaCl was dissolved in the rice seedling culture solution, and seedlings were treated for 14 days, then allowed to recover under normal conditions for 7 days. For polyethylene glycol (PEG) treatment, seedlings were treated with rice seedling culture solution containing 20% PEG-4000 for 14 days and allowed to recover under normal conditions for 7 days.

Map-Based Cloning of *AET1*

The *aet1* mutant was crossed with a *japonica* variety, Jiahua-1, and the F_1 plants were self-pollinated to generate an F_2 mapping population. To fine-map the *AET1* locus, we developed new molecular markers by screening for predicted simple sequence repeats and identified new cleaved amplified polymorphism sequence markers. *AET1* was mapped to a 23.3-kb region on the long arm of chromosome 5, and all DNA fragments from this region were amplified from both *aet1* and wild-type genomic DNA by PCR for DNA sequencing. PCR amplifications were performed using 2× PCR mix (Tiangen #KT207). DNA purification and plasmid DNA extraction were performed using Monarch kits from New England Biolabs (cat. #T1020L and #1010L). The mapping information is shown in Figure 1B, and the PCR primer pairs are listed in Supplemental Table 2.

Plasmid Construction and Plant Transformation

To produce the complementation construct pCAMBIA-1300-*AET1*$_{Pro}$-c*AET1*, we first amplified a 2.5-kb DNA fragment upstream of the *AET1* start codon from TQ genomic DNA, and used TQ cDNA to obtain the full-length *AET1* cDNA. The promoter and cDNA sequences were then cloned into the pCAMBIA1300 vector. The 2.5-kb DNA fragment of the *AET1* upstream region was cloned into the pCAMBIA1300-GUSplus vector to generate the plasmid *AET1*$_{Pro}$:GUS. To generate the overexpression constructs, we amplified the full-length coding sequences of *AET1*, *RACK1A*, and *eIF3h* from TQ and cloned them into the plant binary vectors pCAMBIA1306 and pCAMBIA1301 under the control of the CaMV 35S promoter and the UBI (ubiquitin) promoter, respectively. The CRISPR/Cas9 gene-editing constructs for *AET1*, *RACK1A*, *eIF3h*, and *OsARF23* were designed as previously described (Ma et al., 2015). *Agrobacterium tumefaciens*-mediated transformation of rice was performed as previously described using strain EHA105 (Hiei et al., 1994). All DNA constructs were confirmed by sequencing, and all positive transgenic plants and negative controls were identified by qRT–PCR and hygromycin gene amplification. Specific primers were designed to confirm the mutation positions in each CRISPR/Cas9-positive transgenic line. All plasmid constructs used in this study were generated using NEBuilder HIFI DNA Assembly Master Mix (NEB #E2621L). The PCR primer pairs are listed in Supplemental Table 2.

GUS Staining

GUS staining of *AET1*$_{Pro}$::GUS, *DR5*::GUS/TQ, and *DR5*::GUS/*aet1* transgenic plants was performed as described previously (Wang et al., 2014). Samples were obtained in the field and the laboratory, incubated with GUS staining liquid at 37°C for 12 h, cleared in 75% ethanol to remove chlorophyll, and imaged with a Leica model M205C stereo microscope (Leica Microsystems).

Histochemical Analysis

Plant materials were collected from the field in Shanghai at the tillering stage, fixed in FAA (50% ethanol, 5% glacial acetic acid, 5% formaldehyde) overnight at 4°C, and dehydrated in a graded alcohol series. After fixing with xylene, the samples were embedded in Paraplast (Sigma-Aldrich #P3683) and sliced into 8-μm thin sections with a rotary microtome (Leica RM2126RT). The prepared tissue sections were stained with safranin and then observed under a light microscope (Imager M2; Carl Zeiss).

RNA Extraction and qRT–PCR

Total RNA was extracted from plant tissues using the E.Z.N.A. Total RNA Kit (Omega Bio-Tek #R6834-1). Reverse transcription for qRT–PCR and cDNA synthesis was performed using ReverTra Ace qPCR RT Master Mix with gDNA Remover (Toyobo #FSQ-301) from 200 ng of total RNA. qRT–PCR analysis was performed on the ABI 7300 Real Time PCR System using Fast Start Universal SYBR Green Master Mix with ROX (Roche #4913914001), and the expression data were analyzed using the $2^{-\Delta\Delta Ct}$

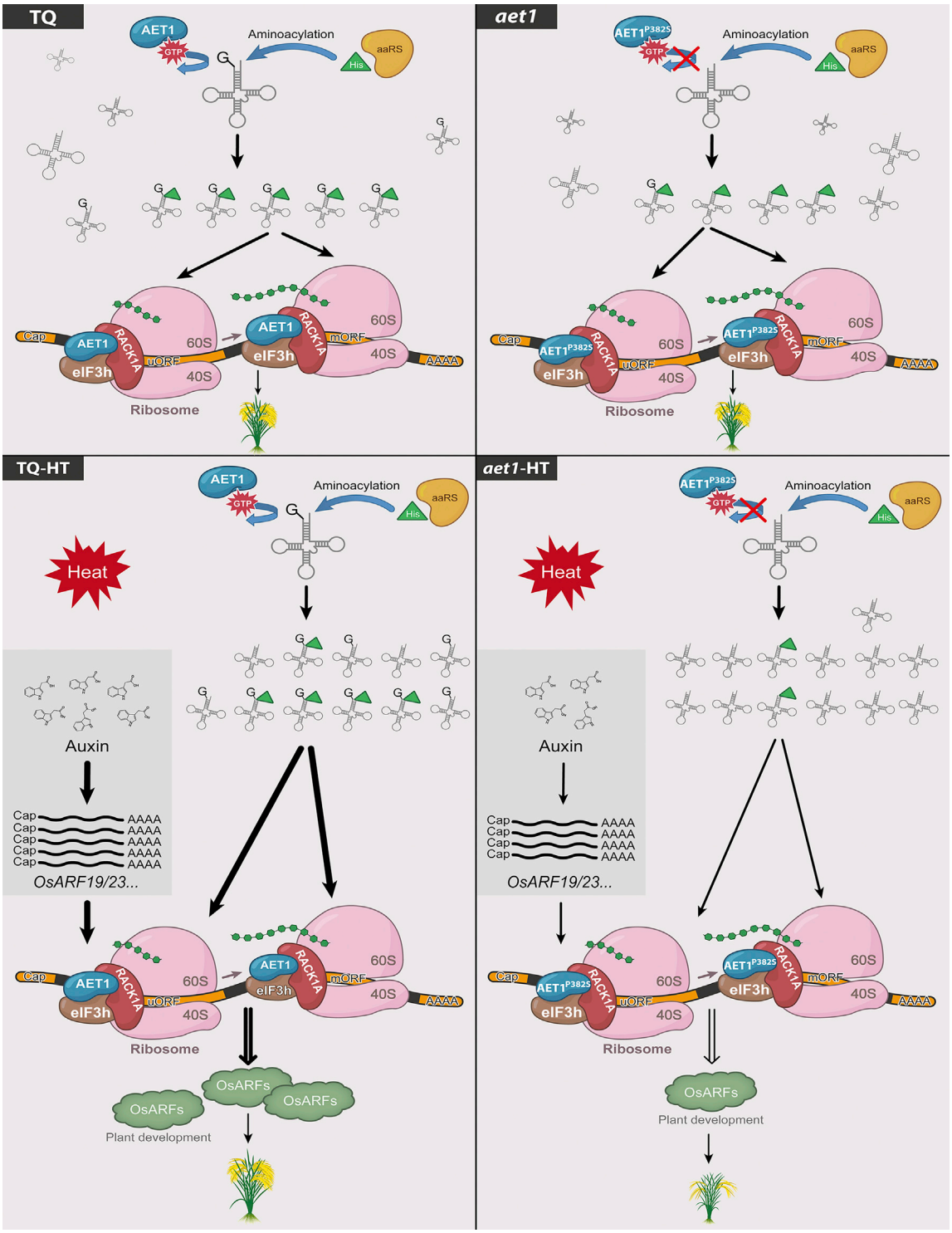

Figure 7. A Working Model to Explain How *AET1* Modulates Auxin Signaling through Translation Regulation Associated with tRNA Modification under High Temperature.

Schematic diagrams showing that AET1 functions as a tRNA modification enzyme and translation regulator together with RACK1A and eIF3h in a temperature-dependent manner. At normal temperatures, the AET1 protein can add a guanosine to the 5′ end of pre-tRNA^{His}, which is then activated and can be recognized by aaRS. Some AET1 proteins are recruited by RACK1A and function with eIF3h to regulate translational efficiency via the binding of AET1 to uORF-containing mRNAs. The *aet1* mutant shows loss of Thg1 enzyme function, leading to reduced aminoacyl-tRNA^{His} levels and translational efficiency. The mutant plants display slight phenotype changes under normal conditions. Under high temperature, AET1 can activate pre-tRNA^{His} and stabilize tRNA homeostasis. In particular, AET1 interacts with RACK1A and eIF3h and associates with the *OsARF19* and *OsARF23* mRNAs, which leads to increased translation of these mRNAs and contributes to plant development in response to high temperature. However, in the *aet1* mutant, the translation of *OsARF19* and *OsARF23* mRNAs is downregulated, which results in reduced levels of OsARFs and eventually causes growth arrest.

method (Livak and Schmittgen, 2001). The *UBQ5* gene was used as the internal reference to normalize gene expression data. All analyses had three biological replicates. PCR primer pairs for gene amplification are listed in Supplemental Table 2.

Protein Expression in *Escherichia coli* and Purification

The full-length cDNA sequence of *AET1* was cloned into the pCOLD-TF (Takara) vector between the *Kpn*I and *Sal*I sites to generate AET1-HIS. The fusion constructs were then introduced into *E. coli* strain BL21 (DE3) pLysS, and the transformants were grown in Luria-Bertani medium containing 100 μg/ml ampicillin at 37°C until OD_{600} = 0.6. Expression of the AET1-HIS fusion protein was induced by addition of 0.5 mM IPTG (isopropyl β-D-1-thiogalactopyranoside) and incubation at 15°C for 24 h. The AET1-HIS protein was purified using PureProteome Nickel Magnetic Beads (cat. #LSKMAGH02) following the manufacturer's instructions. Expression and purification of the $AET1^{P382S}$-HIS protein was also carried out as described above. The full-length *RACK1A* cDNA was cloned into the pMAL-c5x vector, which has an MBP tag between the *Nde*I and *Eco*RI sites, and the recombinant pMAL-c5x vector was then transformed into Rosetta-gami (DE3) competent *E. coli* cells, which were grown to produce fusion proteins as previously described. Amylose resin was used to purify the recombinant proteins (NEB #E8021S). Expression and purification of MBP-eIF3h was also carried out using the same method. All primer sequences are listed in Supplemental Table 2. All restriction enzymes used in this study were obtained from NEB and Fermentas.

tRNA EMSA and Thg1 Enzyme Activity Assay

tDNA information was collected from the genomic tRNA database (http://gtrnadb.ucsc.edu/) (Chan and Lowe, 2016). tDNAs with a T7 promoter were synthesized by Huagene, and we then used the HiScribe T7 High Yield RNA Synthesis Kit (NEB #E2040S) to obtain pure biotin-linked pre-tRNAs. The EMSA/Gel Shift kit (Beyotime #GS002) was used to perform the EMSA, and the Chemiluminescent Nucleic Acid Detection Module (Thermofisher #PI205014) was used to detect the tRNA shift. Biotin antibodies and secondary antibodies (Sigma #B3640 and #A0545) were used, and the detection system was from Tanon 5500. The Thg1 ($tRNA^{His}$ guanylyltransferase) enzyme assay was performed as previously described (Jackman and Phizicky, 2006). [5′-^{32}P]-labeled tRNAs were prepared by phosphorylation with [γ-^{32}P]ATP (PerkinElmer #NEG002Z001MC) using T4 polynucleotide kinase (NEB) to a final activity of 7000 Ci/mmol. The [5′-^{32}P]-labeled tRNA was used as the substrate in a Thg1 assay containing 10 mM $MgCl_2$, 3 mM dithiothreitol (DTT), 123 mM NaCl, 0.2 mg/ml BSA, and 1 mM GTP and ATP. Reactions were carried out at room temperature. After 6 h, the reaction was stopped by transferring an aliquot (4 μl) to a new tube containing 0.5 μl of EDTA and 0.5 μl of 10 mg/ml RNase A (YEASEN #10406ES03). The tubes were incubated for 30 min at 50°C and then treated with 0.5 unit of calf intestinal alkaline phosphatase (YEASEN #20427ES80) in 1× phosphatase reaction buffer in a final volume of 6 μl at 37°C for 30 min. The assays were spotted onto silica gel TLC plates (Merck-Millipore #100384) and resolved in an *n*-propyl alcohol/NH_4OH/H_2O (55:35:10) solvent system. The plates were visualized and quantified with PhosphorImager.

Nucleus Isolation and Ploidy Determination

Isolation of the cell nuclei and assessment of ploidy were performed as described previously (Qi et al., 2012). Seedling root tips 2 cm in length were finely chopped. The samples were resuspended by the nuclear isolation and staining solution (NPE Systems #7216), and the nuclei were stained by the 4′, 6-diamidino-2-phenylindole (DAPI) in the solution. The suspension was later filtered through a 40-μm nylon filter (Thermo Fisher #352340). The nuclei suspension was loaded on a Beckman Moflo cell sorter for flow-cytometric analysis, and the ploidy of approximately 10 000 nuclei/sample was recorded. The relative proportions of G_1, S, and G_2/M phase nuclei were analyzed by FCS Express 4 software.

Subcellular Localization of the AET1, RACK1A, and eIF3h Proteins

To determine the subcellular localization of the AET1, RACK1A, and eIF3h proteins, we cloned the *AET1*, *RACK1A*, and *eIF3h* cDNA fragments separately into the PA7-YFP plasmid and transformed them into *E. coli* competent cells. For all YFP transient expression constructs the *Sal*I and *Sma*I sites were used. After verifying the positive clones by DNA sequencing, the plasmids were extracted and purified from *E. coli* using the Plasmid Maxi Kit (Qiagen #12163). The purified plasmids were used to transfect rice protoplasts. The experiment was performed as previously described (Zhang et al., 2011). Rice protoplasts were made from the fresh shoots of 10-day-old rice seedlings. The shoots were cut into approximately 0.5-mm strips and transferred into 0.6 M D-mannitol (Sigma #78513) solution for 10 min, followed by enzymatic digestion in the dark with gentle shaking for 5 h. Cellulase and macerozyme (Yakult #R-10 and RS) were added to the enzyme digest buffer. The protoplasts were collected by filtration through 100-μm nylon filters (Thermo Fisher #352360). After washing with W5 buffer, a blood counting chamber (Electron Microscopy Sciences #635902) was used to calculate cell numbers, and the protoplasts were then diluted with MMG buffer. We used PEG-mediated transfection to introduce the plasmid DNA, and incubated the rice protoplasts in the dark for 10 h. The fluorescent signals were observed with a Zeiss LSM 880 confocal laser scanning microscope. The ER marker was purchased from The Arabidopsis Information Resource (TAIR; CD3-959) (Nelson et al., 2007).

Yeast Two-Hybrid Screening Assays

Yeast two-hybrid screening assays were performed using the Y2H Gold-Gal4 system (Clontech). Our laboratory had previously constructed two yeast plasmid prey libraries, one from mixed seedlings and the other from mixed spikelets. The libraries were both plasmid based. We cloned the full-length cDNAs into pGBKT7 to form the prey plasmid and then transformed the plasmid into the Y2H Gold strain. The yeast cells were cultured on SD/-Trp medium, and 500-ml cultures were grown to prepare competent cells to transform with the pGADT7 plasmid libraries. After transformation, the yeast cells containing the pGADT7 plasmid libraries were cultured on SD/-Trp-Leu-His or SD/-Trp-Leu-His-Ade medium containing X-α-gal at 30°C for 3 days. SD/-Trp-Leu-His is yeast culture SD medium without tryptophan, leucine, and histidine, and SD/-Trp-Leu-His-Ade is SD medium lacking tryptophan, leucine, histidine, and adenine. The colonies were selected, and the inserts in the pGBKT7 vectors were sequenced. Screening was performed following the manufacturer's (Clontech) instructions.

Yeast Two-Hybrid Assays

Yeast two-hybrid assays were performed with the Y2H Gold-Gal4 system (Clontech). The DNA fragments containing the *AET1*, *RACK1A*, and *eIF3h* coding sequences were cloned separately into the pGBKT7 and pGADT7 vectors to form the bait and prey constructs, respectively. For all pGBKT7 constructs the *Eco*RI and *Sal*I sites were used, while for all pGADT7 constructs the *Eco*RI and *Bam*HI sites were used. All bait and prey constructs were transformed into the yeast Y2H Gold strain as directed by the manufacturer. The yeast cells were cultured on SD/-Trp-Leu-His or SD/-Trp-Leu-His-Ade medium containing X-α-gal at 30°C for 3 days. In the self-activation assays, the SD/-Trp-Leu-His culture medium also contained 5 mM 3-AT. Three biological replicates were performed for all yeast cell dilutions with the same results, and the figures show results for only one experiment. The PCR primers used for the yeast two-hybrid assays are listed in Supplemental Table 2.

Bimolecular Fluorescence Complementation Assays

For the BiFC assays, the *AET1*, *RACK1A*, *eIF3h*, and *OsHAL3* cDNA fragments were cloned into pCAMBIA1300S-YN and pCAMBIA1300S-YC to form the nYFP-protein and cYFP-protein constructs. The plasmids were then transformed into *A. tumefaciens* strain GV3101, and all constructs were verified by DNA sequencing. Leaves of 5-week-old *Nicotiana*

benthamiana plants were co-infiltrated with *A. tumefaciens* strains separately carrying the two constructs. After infiltration the plants were kept in the dark for 48 h, and the BiFC fluorescence signals were then observed using a Zeiss LSM 880 confocal laser scanning microscope (Carl Zeiss). The ER marker used was the pHMS-RFP vector carrying the full-length cDNA of the *AAPT2* gene (AT3G25585). Co-localization of BiFC with the ER marker was observed in leaves of 5-week-old *N. benthamiana* plants using a Leica TSC SP8 STED 3X (Leica Camera AG). PCR primers used for BiFC are listed in Supplemental Table 2.

Pull-Down Assays

The pull-down assays were performed using a previously described method (Cui et al., 2015). *E. coli* cells expressing MBP-RACK1A, MBP-eIF3h, and MBP were disrupted by high-pressure cell disruption (Constant Systems), and centrifuged. The same methods were used for *E. coli* cells expressing the AET1-HIS and pCOLD-TF empty vectors. We incubated the supernatants of the pull-down samples for 2 h at 4°C. The supernatants were then divided into two parts: one part was incubated with Anti-MBP Beads (NEB) and the other was incubated with Ni-NTA (nickel–nitrilotriacetic acid) beads (Takara) for 2 h at 4°C. The beads were washed five times in their respective wash buffers and resuspended in SDS loading buffer. For the MBP bead pull-down samples an anti-His antibody (CWbiotech) was used for detection, and for the samples purified with the Ni-NTA beads an anti-MBP antibody (NEB) was used for detection. For the pull-down assay between RACK1A and eIF3h, the full-length *RACK1A* cDNA was cloned into the pGEX-4T-2 vector and was transformed into BL21 (DE3) competent *E. coli* cells. The pull-down method was similar to that described above, and the supernatants were incubated with Anti-MBP Beads (NEB) and Anti-GST Beads (GE). For the MBP bead pull-down samples an anti-GST antibody (Sigma) was used for detection, and for the samples purified with the Anti-GST beads an anti-MBP antibody (NEB) was used for detection.

tRNA Sequencing

tRNA sequencing was performed by Cloud-Seq Biotech (Shanghai, China). The methods were based on previous studies (Pang et al., 2014; Zheng et al., 2015). Total RNA was isolated from TQ, *aet1*, TQ-HT, and *aet1*-HT seedlings with TRIzol reagent (Invitrogen #15596018) and treated with DNAse (Thermo Scientific #EN0521) to remove contaminating genomic DNA. Ribosomal RNA was depleted with the Ribo-Zero rRNA Removal Kit (Illumina #MRZPL116). The remaining RNA was size-selected for the <200-nt fractions with the MirVana Isolation Kit (Invitrogen #AM1561). The RNA molecules were then de-aminoacylated in 0.1 M Tris–HCl (pH 9.0) and 1 mM EDTA for 30 min at 37°C. tRNA libraries were constructed using the TruSeq Small RNA Preparation Kit (Illumina). All libraries were size-selected (170–210 bp) prior to sequencing on a Hiseq instrument (Illumina). For data analysis, a tRNA library was first adapted from the tRNAScan-SE library by appending CCA to tRNAs from the genomic tRNA database (http://gtrnadb.ucsc.edu/GtRNAdb2/genomes/eukaryota/Osati/). Isodecoders with identical scores were consolidated for ease of identity assignment, decreasing the number of reference genes and pseudogenes from 764 to 321. The raw reads were generated after sequencing, image analysis, base calling, and quality filtering on the Illumina sequencer. A Phred score of Q30 was used to perform quality control. The adaptor sequences were trimmed and the adaptor-trimmed-reads (≥15 nt) were retained using cutadapt software (v1.9.3). The trimmed reads from all samples were then aligned to the tRNA library using bowtie2 software with sensitive options (Langmead and Salzberg, 2012). Mapped reads for each tRNA were counted using samtools (Li et al., 2009). We used edgeR software to detect statistical differences in the expression of tRNAs between conditions (Robinson et al., 2010). All samples had three biological replicates.

RNA Immunoprecipitation Sequencing and Assays

High-throughput sequencing services were provided by Cloud-Seq Biotech (Shanghai, China). Samples from TQ-HT and *aet1*-HT were lysed in an ice-cold lysis buffer, and RIP sequencing was performed as described by Zhao et al. (2008). AET1 antibodies were made by ABclonal (Wuhan, China). RNA was extracted using TRIzol reagent (Invitrogen) following the manufacturer's instructions. rRNAs were removed from the immunoprecipitated RNA and input RNA samples with the Ribo-Zero rRNA Removal Kit (Illumina #MRZPL116). RNA-seq libraries were constructed using rRNA-depleted RNA with the TruSeq Stranded Total RNA Library Prep Kit (Illumina) according to the manufacturer's instructions. The library quality was evaluated with the BioAnalyzer 2100 system (Agilent Technologies, USA). Library sequencing was performed on an Illumina Hiseq instrument with 150-bp paired-end reads. Paired-end read quality was controlled by filtering for Phred scores ≥Q30. After 3′ adaptor-trimming and removal of low-quality reads with cutadapt software (v1.9.3), the high-quality trimmed reads were aligned to the rice reference genome (RAPDB IRGSP-1.0) with hisat2 software (v2.0.4). Next, guided by the gtf gene annotation file, cuffdiff software was used to obtain the gene-level FPKM (fragments per kilobase of transcript per million mapped reads) values for the mRNA expression profiles. Fold changes and *P* values were calculated based on FPKM, and all *P* values were adjusted by false discovery rate correction. The differentially expressed mRNAs were identified (Trapnell et al., 2010). GO (gene ontology) and KEGG pathway enrichment analyses were performed based on the differentially expressed mRNAs. RIP assays were performed using the Magna RIP RNA-Binding Protein Immunoprecipitation Kit (Merck-Millipore #17-700) ollowing the manufacturer's instructions. The cell extracts of TQ-HT and *aet1*-HT were isolated using the RIP kit, and AET1 antibodies bound to the magnetic beads were incubated with the samples. After immunoprecipitation, proteinase K was used to digest proteins. The RNA was then purified from the supernatant. We used a cDNA first-strand synthesis kit to generate cDNAs, then designed PCR primers for the qRT–PCR assays. All immunoprecipitated RNAs were used to synthesize cDNA using ReverTra Ace qPCR RT Master Mix with gDNA Remover (Toyobo #FSQ-301). qRT–PCR analysis was performed on the ABI 7300 Real Time PCR System using Fast Start Universal SYBR Green Master Mix with ROX (Roche #4913914001). The data used specific primers to acquire enriched targets, and Ct values were calculated for the fold enrichment from the enriched targets and immunoglobulin G immunoprecipitated targets.

RNA Electrophoretic Mobility Shift Assay

All probes for use in REMSA were synthesized by Huagene. Cy5 fluorochromes were added to the 5′ ends of the RNA probes. AET1-HIS, AET1^{P382S}-HIS, MBP-RACK1A, and MBP-eIF3h were purified using the methods described above. MBP-GSN1 was used in a previous study as a negative control (Guo et al., 2018). Each binding reaction contained 1× binding buffer, 2.5% glycerol, Cy5-labeled RNA probe, unlabeled RNA probe, and 1 unit protein. The mixtures were then incubated at 30°C or 37°C for 30 min. After incubation, the samples were loaded onto a prepared native polyacrylamide gel and run in 1× TBE buffer at 4°C for 40 min. Gel images were taken using a charge-coupled device camera (Tanon 5500).

Polysome Profiling Assays

Polysome profiling assays were carried out as previously described with some modifications (Zhang et al., 2017). Seven-day-old seedlings grown under normal conditions were transferred to 25°C or 35°C for a further 7 days and were then ground to a fine powder in liquid nitrogen. Tissue samples (3 g) were suspended in 8 ml of pre-chilled 1× ribosome extraction buffer (200 mM Tris–HCl [pH 8.4], 200 mM KCl, 35 mM $MgCl_2$, 2 mM EGTA, 0.5 mg/ml heparin, 25 μg/ml cycloheximide, 100 μg/ml chloramphenicol, 2% Triton X-100, 1% Tween 20, 5 mM DTT, 2% polyethylene oxide, and Protease Inhibitor Cocktail) and incubated on ice for 30 min with gentle mixing to allow for sufficient lysis. Cell debris was discarded after the lysates were centrifuged in a cold bench-top centrifuge for 15 min at 5000 *g* and filtered through a cell strainer (Falcon, 100 μm nylon) to obtain the supernatants. The supernatants were layered on top of a 1.7 M sucrose cushion and centrifuged at 40 000 rpm for 6 h

at 4°C. The ribosome pellets were resuspended in 700 μl of resuspension buffer (200 mM Tris–HCl [pH 9.0], 200 mM KCl, 35 mM $MgCl_2$, 2 mM EGTA, 100 μg/ml chloramphenicol, and 25 μg/ml cycloheximide). The ribosome-containing solutions were layered onto a 9-ml 20%–60% sucrose density gradient and centrifuged at 40 000 rpm for 4 h at 4°C. For each sample, polysomal RNAs were distributed in the sucrose gradient based on the sedimentation coefficient following ultracentrifugation. Each gradient was separated into 700-μl fractions; fractions 1 to 14 containing free mRNA and translationally active mRNA from 40S to the heaviest polysomes were collected and subjected to RNA isolation using TRIzol reagent. For sucrose density gradient preparation, 20%, 30%, 40%, 50%, and 60% (w/v) sucrose solutions were prepared on ice. A 1.8-ml aliquot of 60% sucrose solution was added to a polyallomer centrifuge tube (Beckman) and frozen for 15 min at −80°C. Next, a 1.8-ml aliquot of the 50% sucrose solution was loaded on top of the frozen 60% layer and frozen again, and this process was repeated with 2-ml aliquots of the 40%, 30%, and 20% sucrose solutions. Gradients were stored at −80°C until the day before they were used, at which time they were transferred to 4°C overnight and allowed to thaw slowly and form a continuous density gradient before the samples were loaded for centrifugation.

IAA Measurement

IAA concentration measurements were performed by Metware. High-performance liquid chromatography (HPLC)-grade ACN (acetonitrile) and MeOH (methanol) were purchased from Merck. Milli-Q water (Millipore) was used in all experiments. All standards were purchased from Olchemim and Sigma-Aldrich. Acetic acid was purchased from Sinopharm Chemical Reagent. Stock solutions of the standards were prepared at a concentration of 10 mg/ml in ACN. All stock solutions were stored at −20°C. The stock solutions were diluted with ACN to working concentrations prior to analysis. Fresh plant materials were harvested, weighed, flash frozen in liquid nitrogen, and stored at −80°C until needed. Plant tissues (120 mg fresh weight) were ground into powder in a mortar with liquid nitrogen and extracted with methanol/water (8:2) at 4°C. The extracts were centrifuged at 12 000 *g* at 4°C for 15 min. The supernatants were collected and then evaporated to dryness under a nitrogen gas stream, and reconstituted in methanol/water (3:7). The solutions were centrifuged and the supernatants were collected for liquid chromatography–mass spectrometry (LC–MS) analysis. The sample extracts were analyzed using an LC–electrospray ionization (ESI)–MS/MS system (HPLC, Shim-pack UFLC Shimadzu CBM30A system, www.shimadzu.com.cn/; MS, Applied Biosystems 6500 Triple Quadrupole, www.appliedbiosystems.com.cn/). The analytical conditions for HPLC were as follows: column, Waters ACQUITY UPLC HSS T3 C18 (1.8 μm, 2.1 × 100 mm); solvent system, water (0.04% acetic acid): acetonitrile (0.04% acetic acid); gradient program, 95:5 v/v at 0 min, 5:95 v/v at 11.0 min, 5:95 v/v at 12.0 min, 95:5 v/v at 12.1 min, 95:5 v/v at 15.0 min; flow rate, 0.35 ml/min; temperature, 40°C; injection volume, 5 μl. The effluent was alternatively connected to a Q TRAP (ESI-triple quadrupole-linear ion trap)-MS and an API 6500 Q TRAP LC/MS/MS system, equipped with an ESI Turbo Ion-Spray interface, operating in a positive ion mode and controlled by Analyst 1.6 software (AB Sciex). The ESI source operation parameters were as follows: ion source, turbo spray; source temperature, 500°C; ion-spray voltage, 5500 V; curtain gas was set at 35.0 psi; the collision gas was medium. Declustering potential (DP) and collision energy (CE) for individual multiple reaction monitoring (MRM) transitions was done with further DP and CE optimization. A specific set of MRM transitions was monitored for each period based on the amount of IAA eluted.

ACCESSION NUMBERS

Sequence data from this article were downloaded from TAIR and the MSU rice annotation database/Gramene/RAPDB under the following accession numbers: LOC_Os05g45890, Os05g0535500 (*AET1*); LOC_Os01g49290, Os01g0686800 (*RACK1A*); LOC_Os04g30780, Os04g0376500 (*eIF3h*); LOC_Os07g42450, Os07g0616600 (*Ribosomal Protein S2*); LOC_Os06g48950, Os06g0702600 (*OsARF19*); LOC_Os11g32110, Os11g0523800 (*OsARF23*); AT3G25585 (*AAPT2*).

SUPPLEMENTAL INFORMATION

Supplemental Information is available at *Molecular Plant Online*.

FUNDING

This work was supported by the grants from National Natural Science Foundation of China (31630052, 31788103), the Ministry of Science and Technology of China (2016YFD0100902, 2016YFD0100604), Chinese Academy of Sciences (QYZDY-SSW-SMC023, XDB27010104), the Shanghai Science and Technology Development (18JC1415000), CAS-Croucher Funding Scheme for Joint Laboratories, and National Key Laboratory of Plant Molecular Genetics, China.

AUTHOR CONTRIBUTIONS

H.-X.L. conceived and supervised the project, and H.-X.L., J.-X.S., K.C., T.G., and X.-M.L. designed the experiments. K.C., T.G., and X.-M.L. performed most of the experiments. Y.-M.Z., Y.-B.Y., W.-W.Y., N.-Q.D., C.-L.S., Y.K., Y.-H.X., H.Z., Y.-C.L., J.-P.G., X.H., Q.Z., B.H., J.-X.S. and H.-X.L. performed some of the experiments. K.C., T.G., and H.-X.L. analyzed data and wrote the manuscript.

ACKNOWLEDGMENTS

We thank Min Shi (Institute of Plant Physiology and Ecology, SIBS, CAS) for technical support for the transgenic assay. We thank Xiaoshu Gao, Xiaoyan Gao, Zhiping Zhang, Jiqin Li, Naixu Xu, and Wenfang Zhao (Institute of Plant Physiology and Ecology, SIBS, CAS) for technical support. We thank Professor Yaoguang Liu (South China Agriculture University) for donation of CRISPR/Cas9 plasmids. We thank Professor Hongwei Xue (Shanghai Institute of Plant Physiology and Ecology, CAS) for DR5 transgenic lines seed donation. We thank Professor Dabing Zhang (Shanghai Jiao Tong University) for donation of *OsARF23* antibody. We thank Chunjie Cao (Carl Zeiss) for X-ray microscope observation. No conflict of interest declared.

Received: October 13, 2018
Revised: April 11, 2019
Accepted: April 29, 2019
Published: May 6, 2019

REFERENCES

Bita, C.E., and Gerats, T. (2013). Plant tolerance to high temperature in a changing environment: scientific fundamentals and production of heat stress-tolerant crops. Front. Plant Sci. **4**:273.

Browning, K.S., and Bailey-Serres, J. (2015). Mechanism of cytoplasmic mRNA translation. *Arabidopsis* Book **13**:e0176.

Chan, P.P., and Lowe, T.M. (2016). GtRNAdb 2.0: an expanded database of transfer RNA genes identified in complete and draft genomes. Nucleic Acids Res. **44**:D184–D189.

Chen, J.G., Ullah, H., Temple, B., Liang, J., Guo, J., Alonso, J.M., Ecker, J.R., and Jones, A.M. (2006). RACK1 mediates multiple hormone responsiveness and developmental processes in *Arabidopsis*. J. Exp. Bot. **57**:2697–2708.

Chen, P., Jager, G., and Zheng, B. (2010). Transfer RNA modifications and genes for modifying enzymes in *Arabidopsis thaliana*. BMC Plant Biol. **10**:201.

Cortijo, S., Charoensawan, V., Brestovitsky, A., Buning, R., Ravarani, C., Rhodes, D., van Noort, J., Jaeger, K.E., and Wigge, P.A. (2017). Transcriptional regulation of the ambient temperature response by H2A.Z nucleosomes and HSF1 transcription factors in *Arabidopsis*. Mol. Plant **10**:1258–1273.

Cui, L.G., Shan, J.X., Shi, M., Gao, J.P., and Lin, H.X. (2015). DCA1 Acts as a transcriptional co-activator of DST and contributes to drought and salt tolerance in rice. PLoS Genet. **11**:e1005617.

Franklin, K.A., Lee, S.H., Patel, D., Kumar, S.V., Spartz, A.K., Gu, C., Ye, S., Yu, P., Breen, G., Cohen, J.D., et al. (2011). Phytochrome-interacting factor 4 (PIF4) regulates auxin biosynthesis at high temperature. Proc. Natl. Acad. Sci. U S A **108**:20231–20235.

Gomes-Duarte, A., Lacerda, R., Menezes, J., and Romao, L. (2018). eIF3: a factor for human health and disease. RNA Biol. **15**:26–34.

Gunisova, S., Hronova, V., Mohammad, M.P., Hinnebusch, A.G., and Valasek, L.S. (2018). Please do not recycle! Translation reinitiation in microbes and higher eukaryotes. FEMS Microbiol. Rev. **42**:165–192.

Guo, J., Wang, J., Xi, L., Huang, W.D., Liang, J., and Chen, J.G. (2009). RACK1 is a negative regulator of ABA responses in *Arabidopsis*. J. Exp. Bot. **60**:3819–3833.

Guo, T., Chen, K., Dong, N.Q., Shi, C.L., Ye, W.W., Gao, J.P., Shan, J.X., and Lin, H.X. (2018). GRAIN SIZE AND NUMBER1 negatively regulates the OsMKKK10-OsMKK4-OsMPK6 cascade to coordinate the trade-off between grain number per panicle and grain size in rice. Plant Cell **30**:871–888.

He, W., Brumos, J., Li, H., Ji, Y., Ke, M., Gong, X., Zeng, Q., Li, W., Zhang, X., An, F., et al. (2011). A small-molecule screen identifies L-kynurenine as a competitive inhibitor of TAA1/TAR activity in ethylene-directed auxin biosynthesis and root growth in *Arabidopsis*. Plant Cell **23**:3944–3960.

Hiei, Y., Ohta, S., Komari, T., and Kumashiro, T. (1994). Efficient transformation of rice (*Oryza sativa* L.) mediated by *Agrobacterium* and sequence analysis of the boundaries of the T-DNA. Plant J. **6**:271–282.

Hinnebusch, A.G. (2014). The scanning mechanism of eukaryotic translation initiation. Annu. Rev. Biochem. **83**:779–812.

Hinnebusch, A.G., and Lorsch, J.R. (2012). The mechanism of eukaryotic translation initiation: new insights and challenges. Cold Spring Harb. Perspect. Biol. **4**:a011544.

Huang, X., Zhao, Y., Wei, X., Li, C., Wang, A., Zhao, Q., Li, W., Guo, Y., Deng, L., Zhu, C., et al. (2011). Genome-wide association study of flowering time and grain yield traits in a worldwide collection of rice germplasm. Nat. Genet. **44**:32–39.

Jackman, J.E., and Phizicky, E.M. (2006). $tRNA^{His}$ guanylyltransferase catalyzes a 3'-5' polymerization reaction that is distinct from G_{-1} addition. Proc. Natl. Acad. Sci. U S A **103**:8640–8645.

Jaya, N., Garcia, V., and Vierling, E. (2009). Substrate binding site flexibility of the small heat shock protein molecular chaperones. Proc. Natl. Acad. Sci. U S A **106**:15604–15609.

Jin, X., Lv, Z., Gao, J., Zhang, R., Zheng, T., Yin, P., Li, D., Peng, L., Cao, X., Qin, Y., et al. (2018). AtTrm5a catalyses 1-methylguanosine and 1-methylinosine formation on tRNAs and is important for vegetative and reproductive growth in *Arabidopsis thaliana*. Nucleic Acids Res. **47**:883–898.

Kim, B.H., Cai, X., Vaughn, J.N., and von Arnim, A.G. (2007). On the functions of the h subunit of eukaryotic initiation factor 3 in late stages of translation initiation. Genome Biol. **8**:R60.

Kim, T.H., Kim, B.H., Yahalom, A., Chamovitz, D.A., and von Arnim, A.G. (2004). Translational regulation via 5' mRNA leader sequences revealed by mutational analysis of the *Arabidopsis* translation initiation factor subunit eIF3h. Plant Cell **16**:3341–3356.

Kouba, T., Rutkai, E., Karaskova, M., and Valasek, L. (2012). The eIF3c/NIP1 PCI domain interacts with RNA and RACK1/ASC1 and promotes assembly of translation preinitiation complexes. Nucleic Acids Res. **40**:2683–2699.

Kumar, S., Stecher, G., and Tamura, K. (2016). MEGA7: molecular evolutionary genetics analysis version 7.0 for bigger datasets. Mol. Biol. Evol. **33**:1870–1874.

Kumar, S.V., and Wigge, P.A. (2010). H2A.Z-containing nucleosomes mediate the thermosensory response in *Arabidopsis*. Cell **140**:136–147.

Langmead, B., and Salzberg, S.L. (2012). Fast gapped-read alignment with Bowtie 2. Nat. Methods **9**:357–359.

Letunic, I., and Bork, P. (2016). Interactive tree of life (iTOL) v3: an online tool for the display and annotation of phylogenetic and other trees. Nucleic Acids Res. **44**:W242–W245.

Li, G., Liang, W., Zhang, X., Ren, H., Hu, J., Bennett, M.J., and Zhang, D. (2014). Rice actin-binding protein RMD is a key link in the auxin-actin regulatory loop that controls cell growth. Proc. Natl. Acad. Sci. U S A **111**:10377–10382.

Li, H., Handsaker, B., Wysoker, A., Fennell, T., Ruan, J., Homer, N., Marth, G., Abecasis, G., Durbin, R., and Genome Project Data Processing, S. (2009). The sequence alignment/map format and SAMtools. Bioinformatics **25**:2078–2079.

Lian, X., Guo, J., Gu, W., Cui, Y., Zhong, J., Jin, J., He, Q.Y., Wang, T., and Zhang, G. (2016). Genome-wide and experimental resolution of relative translation elongation speed at individual gene level in human cells. PLoS Genet. **12**:e1005901.

Liu, Y., Wang, G., and Wang, X. (2015). Role of aminoalcoholphosphotransferases 1 and 2 in phospholipid homeostasis in *Arabidopsis*. Plant Cell **27**:1512–1528.

Livak, K.J., and Schmittgen, T.D. (2001). Analysis of relative gene expression data using real-time quantitative PCR and the 2(-Delta Delta C(T)) method. Methods **25**:402–408.

Ma, X., Zhang, Q., Zhu, Q., Liu, W., Chen, Y., Qiu, R., Wang, B., Yang, Z., Li, H., Lin, Y., et al. (2015). A robust CRISPR/Cas9 system for convenient, high-efficiency multiplex genome editing in monocot and dicot plants. Mol. Plant **8**:1274–1284.

Merchante, C., Stepanova, A.N., and Alonso, J.M. (2017). Translation regulation in plants: an interesting past, an exciting present and a promising future. Plant J. **90**:628–653.

Nelson, B.K., Cai, X., and Nebenführ, A. (2007). A multicolored set of in vivo organelle markers for co-localization studies in *Arabidopsis* and other plants. Plant J. **51**:1126–1136.

Nielsen, M.H., Flygaard, R.K., and Jenner, L.B. (2017). Structural analysis of ribosomal RACK1 and its role in translational control. Cell Signal. **35**:272–281.

Pang, Y.L., Abo, R., Levine, S.S., and Dedon, P.C. (2014). Diverse cell stresses induce unique patterns of tRNA up- and down-regulation: tRNA-seq for quantifying changes in tRNA copy number. Nucleic Acids Res. **42**:e170.

Qi, P., Lin, Y.-S., Song, X.-J., Shen, J.-B., Huang, W., Shan, J.-X., Zhu, M.-Z., Jiang, L., Gao, J.-P., and Lin, H.-X. (2012). The novel quantitative trait locus GL3.1 controls rice grain size and yield by regulating Cyclin-T1;3. Cell Res. **22**:1666–1680.

Robinson, M.D., McCarthy, D.J., and Smyth, G.K. (2010). edgeR: a Bioconductor package for differential expression analysis of digital gene expression data. Bioinformatics **26**:139–140.

Rosado, A., Li, R., van de Ven, W., Hsu, E., and Raikhel, N.V. (2012). *Arabidopsis* ribosomal proteins control developmental programs through translational regulation of auxin response factors. Proc. Natl. Acad. Sci. U S A **109**:19537–19544.

Roy, B., Vaughn, J.N., Kim, B.H., Zhou, F., Gilchrist, M.A., and Von Arnim, A.G. (2010). The h subunit of eIF3 promotes reinitiation competence during translation of mRNAs harboring upstream open reading frames. RNA **16**:748–761.

Sasaki, T., and Burr, B. (2000). Sasaki and Burr, 2000-International Rice Genome Sequencing Project, the effect to complete sequence the rice genome. Curr. Opin. Plant Biol. **3**:138–141.

Schepetilnikov, M., Dimitrova, M., Mancera-Martinez, E., Geldreich, A., Keller, M., and Ryabova, L.A. (2013). TOR and S6K1 promote translation reinitiation of uORF-containing mRNAs via phosphorylation of eIF3h. EMBO J. **32**:1087–1102.

Schepetilnikov, M., and Ryabova, L.A. (2017). Auxin signaling in regulation of plant translation reinitiation. Front. Plant Sci. **8**:1014.

Schepetilnikov, M., and Ryabova, L.A. (2018). Recent discoveries on the role of TOR (Target of Rapamycin) signaling in translation in plants. Plant Physiol. **176**:1095–1105.

Sengupta, J., Nilsson, J., Gursky, R., Spahn, C.M., Nissen, P., and Frank, J. (2004). Identification of the versatile scaffold protein RACK1 on the eukaryotic ribosome by cryo-EM. Nat. Struct. Mol. Biol. **11**:957–962.

Thakor, N., Smith, M.D., Roberts, L., Faye, M.D., Patel, H., Wieden, H.J., Cate, J.H.D., and Holcik, M. (2017). Cellular mRNA recruits the ribosome via eIF3-PABP bridge to initiate internal translation. RNA Biol. **14**:553–567.

Trapnell, C., Williams, B.A., Pertea, G., Mortazavi, A., Kwan, G., van Baren, M.J., Salzberg, S.L., Wold, B.J., and Pachter, L. (2010). Transcript assembly and quantification by RNA-Seq reveals unannotated transcripts and isoform switching during cell differentiation. Nat. Biotechnol. **28**:511–515.

Ueda, K., Matsuura, H., Yamaguchi, M., Demura, T., and Kato, K. (2012). Genome-wide analyses of changes in translation state caused by elevated temperature in *Oryza sativa*. Plant Cell Physiol. **53**:1481–1491.

Wang, H.L., and Chekanova, J.A. (2016). Small RNAs: essential regulators of gene expression and defenses against environmental stresses in plants. Wiley Interdiscip. Rev. RNA **7**:356–381.

Wang, M., Zhang, Q., Liu, F.C., Xie, W.F., Wang, G.D., Wang, J., Gao, Q.H., and Duan, K. (2014). Family-wide expression characterization of *Arabidopsis* beta-carbonic anhydrase genes using qRT-PCR and Promoter::GUS fusions. Biochimie **97**:219–227.

Wang, Y., Li, D., Gao, J., Li, X., Zhang, R., Jin, X., Hu, Z., Zheng, B., Persson, S., and Chen, P. (2017a). The 2'-O-methyladenosine nucleoside modification gene OsTRM13 positively regulates salt stress tolerance in rice. J. Exp. Bot. **68**:1479–1491.

Wang, Y., Pang, C., Li, X., Hu, Z., Lv, Z., Zheng, B., and Chen, P. (2017b). Identification of tRNA nucleoside modification genes critical for stress response and development in rice and *Arabidopsis*. BMC Plant Biol. **17**:261.

Wang, Y., Wang, C., Zheng, M., Lyu, J., Xu, Y., Li, X., Niu, M., Long, W., Wang, D., Wang, H., et al. (2016). WHITE PANICLE1, a Val-tRNA synthetase regulating chloroplast ribosome biogenesis in rice, is essential for early chloroplast development. Plant Physiol. **170**:2110–2123.

Wigge, P.A. (2013). Ambient temperature signalling in plants. Curr. Opin. Plant Biol. **16**:661–666.

Xie, X., Guo, P., Yu, H., Wang, Y., and Chen, G. (2018). Ribosomal proteins: insight into molecular roles and functions in hepatocellular carcinoma. Oncogene **37**:277–285.

Xu, G., Yuan, M., Ai, C., Liu, L., Zhuang, E., Karapetyan, S., Wang, S., and Dong, X. (2017). uORF-mediated translation allows engineered plant disease resistance without fitness costs. Nature **545**:491–494.

Xu, J., Zhang, B., Jiang, C., and Ming, F. (2011). RceIF5A, encoding an eukaryotic translation initiation factor 5A in Rosa chinensis, can enhance thermotolerance, oxidative and osmotic stress resistance of *Arabidopsis thaliana*. Plant Mol. Biol. **75**:167–178.

Zhang, H., Si, X., Ji, X., Fan, R., Liu, J., Chen, K., Wang, D., and Gao, C. (2018). Genome editing of upstream open reading frames enables translational control in plants. Nat. Biotechnol. **36**:894–898.

Zhang, L., Liu, X., Gaikwad, K., Kou, X., Wang, F., Tian, X., Xin, M., Ni, Z., Sun, Q., Peng, H., et al. (2017). Mutations in eIF5B confer thermosensitive and pleiotropic phenotypes via translation defects in *Arabidopsis thaliana*. Plant Cell **29**:1952–1969.

Zhang, Y., Su, J., Duan, S., Ao, Y., Dai, J., Liu, J., Wang, P., Li, Y., Liu, B., Feng, D., et al. (2011). A highly efficient rice green tissue protoplast system for transient gene expression and studying light/chloroplast-related processes. Plant Methods **7**:30.

Zhao, J., Sun, B.K., Erwin, J.A., Song, J.J., and Lee, J.T. (2008). Polycomb proteins targeted by a short repeat RNA to the mouse X chromosome. Science **322**:750–756.

Zhao, Q., Feng, Q., Lu, H., Li, Y., Wang, A., Tian, Q., Zhan, Q., Lu, Y., Zhang, L., Huang, T., et al. (2018). Pan-genome analysis highlights the extent of genomic variation in cultivated and wild rice. Nat. Genet. **50**:278–284.

Zheng, G., Qin, Y., Clark, W.C., Dai, Q., Yi, C., He, C., Lambowitz, A.M., and Pan, T. (2015). Efficient and quantitative high-throughput tRNA sequencing. Nat. Methods **12**:835–837.

Zhou, F., Roy, B., and von Arnim, A.G. (2010). Translation reinitiation and development are compromised in similar ways by mutations in translation initiation factor eIF3h and the ribosomal protein RPL24. BMC Plant Biol. **10**:193.

Zhou, W., Karcher, D., and Bock, R. (2013). Importance of adenosine-to-inosine editing adjacent to the anticodon in an *Arabidopsis* alanine tRNA under environmental stress. Nucleic Acids Res. **41**:3362–3372.

Zhu, W., Ausin, I., Seleznev, A., Mendez-Vigo, B., Pico, F.X., Sureshkumar, S., Sundaramoorthi, V., Bulach, D., Powell, D., Seemann, T., et al. (2015). Natural variation identifies *ICARUS1*, a universal gene required for cell proliferation and growth at high temperatures in *Arabidopsis thaliana*. PLoS Genet. **11**:e1005085.